Title

Multireceptor phage cocktail against Salmonella enterica to circumvent phage resistance

Permalink

https://escholarship.org/uc/item/5k96g0m6

Authors

Martinez-Soto, Carlos E
McClelland, Michael
Kropinski, Andrew M
et al.

Publication Date

DOI

Peer reviewed

Multireceptor phage cocktail against *Salmonella enterica* to circumvent phage resistance

Carlos E. Martinez-Soto[1,2], Michael McClelland[3], Andrew M. Kropinski[4], Janet T. Lin[1], Cezar M. Khursigara [ID][2,*], Hany Anany[1,2,*]

[1]Guelph Research and Development Centre, Agriculture and Agri-Food Canada, 93 Stone Rd W, N1G 5C9, Guelph, Ontario, Canada
[2]Department of Molecular and Cellular Biology, College of Biological Science, University of Guelph, 50 Stone Rd E, N1G 2W1, Guelph, Ontario, Canada
[3]Department of Microbiology and Molecular Genetics, School of Medicine, University of California, Irvine, 811 Health Sciences Road, CA 92614, United States
[4]Department of Pathobiology, Ontario Veterinary College, University of Guelph, Guelph, 419 Gordon St, Guelph, ON N1G 2W1, Canada
*Corresponding author. Department of Molecular and Cellular Biology, College of Biological Science, University of Guelph, 50 Stone Rd E, N1G 2W1, Guelph, Ontario, Canada. Email: ckhursig@uoguelph.ca, Guelph Research and Development Centre, Agriculture and Agri-Food Canada, 93 Stone Rd W, N1G 5C9, Guelph, Ontario, Canada. Email: hany.anany@agr.gc.ca
Editor: [Carmen Buchrieser]

Abstract

Non-Typhoidal *Salmonella* (NTS) is one of the most common food-borne pathogens worldwide, with poultry products being the major vehicle for pathogenesis in humans. The use of bacteriophage (phage) cocktails has recently emerged as a novel approach to enhancing food safety. Here, a multireceptor *Salmonella* phage cocktail of five phages was developed and characterized. The cocktail targets four receptors: O-antigen, BtuB, OmpC, and rough *Salmonella* strains. Structural analysis indicated that all five phages belong to unique families or subfamilies. Genome analysis of four of the phages showed they were devoid of known virulence or antimicrobial resistance factors, indicating enhanced safety. The phage cocktail broad antimicrobial spectrum against *Salmonella*, significantly inhibiting the growth of all 66 strains from 20 serovars tested *in vitro*. The average bacteriophage insensitive mutant (BIM) frequency against the cocktail was 6.22×10^{-6} in S. Enteritidis, significantly lower than that of each of the individual phages. The phage cocktail reduced the load of *Salmonella* in inoculated chicken skin by 3.5 $\log_{10}$ CFU/cm^2 after 48 h at 25°C and 15°C, and 2.5 $\log_{10}$ CFU/cm^2 at 4°C. A genome-wide transduction assay was used to investigate the transduction efficiency of the selected phage in the cocktail. Only one of the four phages tested could transduce the kanamycin resistance cassette at a low frequency comparable to that of phage P22. Overall, the results support the potential of cocktails of phage that each target different host receptors to achieve complementary infection and reduce the emergence of phage resistance during biocontrol applications.

Keywords: bacteriophage biocontrol; bacteriophage receptors; *Salmonella* phages; phage resistance; phage food safety; bacteriophage cocktails

Importance

Salmonella enterica subsp. *enterica* is one of the most prevalent food-borne bacterial pathogens with the highest incidence reported in poultry. Lytic phages have been proposed as natural antimicrobials in different settings including food disinfection. The ability of lytic phages to infect and lyse their bacterial target with high specificity makes them ideal candidates for pathogen biocontrol in food production. However, some hurdles exist to exploiting phage technology for biocontrol purposes to enhance food safety such as the high variability in *Salmonella enteritca* and rapid development of phage resistant mutants. In this study, a systematic phage cocktail design was employed to overcome these hurdles. The cocktail not only has a broad spectrum but also minimizes the emergence of phage resistance *in vitro* and on chicken skin holding a great promise as a biocontrol tool against *Salmonella*, making it a valuable addition to poultry processing practices for enhanced food safety.

Introduction

Non-Typhoidal *Salmonella* (NTS) is a Gram-negative rod-shaped flagellated nonspore-forming bacterium that belongs to the fam-ily *Enterobacteriaceae* (Su and Chiu 2007). NTS ranks among the top three foodborne pathogens in terms of illnesses, hospitaliza-tions, and deaths (CDC 2023). NTS accounts for ∼94 million cases of illness and 155 000 deaths every year worldwide (Sher et al. 2021). Furthermore, the economic burden due to *Salmonella* in-fections and contamination of food products has been estimated at $4.1 billion and $287 million annually in USA and Canada, respectively (Jain et al. 2019, Economic Research Service 2022). Poultry meat and derived products account for 19% and 16% of NTS illness cases, and outbreaks reported yearly, respectively (Thomas et al. 2015, CDC 2020a). Due to this high prevalence, numerous outbreaks linked to poultry products have been re-ported in USA, Canada, and elsewhere leading to significant eco-nomic losses (Hoffmann et al. 2012, Thomas et al. 2013, 2015, Basler et al. 2016, Emond-Rheault et al. 2017). NTS infection of birds in farms results in asymptomatic cecal colonization caus-ing persistent shedding of the bacteria throughout the produc-tion chain (Harvey et al. 2011). A strategy to prevent this colo-nization is the administration of live attenuated and killed vac-cines, which have shown high efficacy and are now manda-tory in the EU against S. against S. Enteritidis and Typhimurium (Theuß et al. 2018). Moreover, during processing, traditional meth-

ods to mitigate contamination and reduce *Salmonella* loads on poultry rely on chemical and physical antimicrobial interventions (Islam et al. 2021). For chemical interventions (e.g. chlorine) factors such as insufficient contact time, diffusion, and inactivation can render them ineffective (Islam et al. 2021). Furthermore, the exposure of *Salmonella* to subinhibitory concentrations of these chemicals supports the emergence of disinfectant-tolerant, antibiotic-resistant bacteria (Ortega Morente et al. 2013). On the other hand, physical treatments (e.g. high, pressure processing) not only can cause undesirable effects on the organoleptic properties of poultry but also require expensive equipment and rigorous personnel training, which increase the production costs (Kruk et al. 2014, Moye et al. 2018, Radovčić et al. 2019).

Phages are naturally occurring viruses that specifically infect bacteria (Salmond and Fineran 2015). The ability of lytic phages to infect and lyse their bacterial target with high specificity makes them ideal candidates for therapy and biocontrol (Lin et al. 2017, Islam et al. 2019). In food processing, phages can applied as sanitizers to clean food contact surfaces and equipment, directly on the food products as decontamination agents, and to prevent the growth of pathogenic and spoilage bacteria in packaged food products (Moye et al. 2018, El-Dougdoug et al. 2019). Numerous recent studies have shown the efficacy of experimental (Goode et al. 2003, Whichard et al. 2003, Higgins et al. 2005, Guenther et al. 2009, Hungaro et al. 2013, Kang et al. 2013, Spricigo et al. 2013, Zinno et al. 2014, Islam et al. 2019, Atterbury et al. 2020) and commercial (Sukumaran et al. 2015, Grant et al. 2017, Clavijo et al. 2019, Phagelux 2020) phage formulations to reduce and control the growth of *Salmonella* in raw poultry meat and ready-to-eat products. However, despite their promising features, many hurdles exist to exploiting phage technology for biocontrol purposes. For instance, selecting an adequate phage requires extensive screening and characterization. A basic understanding of the phage biological features such as; replication cycle, presence of bacterial virulence or antimicrobial resistance genes (AMR), infection kinetics, transduction rates, and the emergence of phage resistance is critical to ensure the efficacy and safety of their application (Islam et al. 2021). In addition, most of the recent studies regarding *Salmonella* phages focus on highly prevalent serovars while overlooking less prevalent serovars often associated with outbreaks (CDC 2020b). Since *Salmonella* encompasses over 1 547 serovars, developing a phage-based product that can target the most common and rare serovars is a challenge (Ferrari et al. 2019). Another challenge for phage biocontrol is the emergence of phage resistance in bacteria. Phage resistance mechanisms are widespread across *S. enterica* serovars, including receptor modification, retrons, restriction–modification (R–M) and CRISPR–Cas systems, receptor masking, and repression by prophages (Fox et al. 2007, Santander and Robeson 2007, Shariat et al. 2015, Bai et al. 2019, Wahl et al. 2019, Wang et al. 2019, Millman et al. 2020). Phage application during food processing can lyse susceptible bacteria and select naturally occurring bacteriophage-insensitive mutants (BIMs). These BIMs can perdure in the food production chain and potentially reach the final consumer (Islam et al. 2021). Strategies to overcome these challenges include the rational design of phage cocktails and the use of genetically modified phages (Yehl et al. 2019, Gao et al. 2022). In the context of phage applications in foods, the preference for natural phages over genetically modified counterparts is driven by considerations such as regulatory approval and consumer acceptance (Moye et al. 2018). Naturally occurring lytic phage cocktails can be strategically designed with key attributes including: (1) a broad host range, (2) genetic distinctiveness, (3) unique receptors, and (4) layering of phages. Such designs have been implemented to expand the host range and decrease phage resistance emergence (Kim et al. 2014, Bai et al. 2019, El-Dougdoug et al. 2019, Hesse et al. 2020). This study aimed to develop a genomically distinct, multi-receptor phage cocktail against *Salmonella* following a systematic phage characterization pipeline and evaluate its efficacy to minimize resistance emergence and the growth of multiple *Salmonella* serovars.

Material and methods

Bacterial strains and growth conditions

A total of 66 *S. enterica* subsp. *enterica* strains were used in this study for bacteriophage host range determination and isolation (Table S1, Supporting Information). All strains were stored at −80°C in 25% (v/v) glycerol. To prepare a working overnight culture, a loopful from the frozen culture was streaked out on Tryptic Soy Agar (TSA, Difco™, BD, USA) and incubated overnight at 37°C. Then, a single colony was used to inoculate Tryptic Soy Broth (TSB, Difco™) and incubated overnight at 37°C. Bacterial lawns were prepared as previously described (Kropinski et al. 2009). Briefly, 100 μl of a *Salmonella* overnight culture were added to 5 ml of molten (55°C) soft agar (TSB, 0.5% agar) and immediately poured onto TSA (Difco™) plates. These were allowed to solidify for 20 min and further spotted with respective bacteriophage dilutions.

Sample processing for phage enrichment

A total of 60 samples were used for isolation of *Salmonella* phages, including, sewage (primary sludge, Guelph, Fergus, Hamilton, and Waterloo, wastewater treatment plants, Ontario, Canada), retail duck and chicken skin, chicken and geese feces, chicken and turkey feathers, run-off water from poultry processing plants, and river water (Speed River, Guelph, Ontario, Canada). Samples were processed differently according to their physical nature. For solid samples (e.g. chicken skin) ∼10 g of sample was mixed with 10 ml of 2X TSB, the sample was immediately enriched as described in section 2.3. Semisolid samples (e.g. primary sludge) were processed as previously described (Yu et al. 2016). Briefly, primary sludge was incubated with 50 mM tetrasodium pyrophosphate ($Na_4P_2O_7$, Thermo Fisher Scientific™) at room temperature with moderate agitation and centrifuged at 10 000 × g for 10 min. Supernatant was then filtered using 0.45-μm syringe filter (BD Luer-Lok™). A volume of 10 ml of the filtrate was mixed with 10 ml of 2X TSB and the sample was enriched as described in section 2.3. Liquid samples (e.g. river water) were centrifuged at 10 000 × g for 10 min and filtered using a 0.45-μm syringe filter. A total of 10 ml of the filtrate were mixed with 10 ml of 2X TSB, samples were then enriched as described below.

Sample enrichment for phage isolation

Bacteriophages were isolated using three different enrichment methods; (1) single strain (SS), (2) cocktail of strains (CE), and (3) cyclic sequential (CS) as previously described (Martinez-Soto et al. 2021). For SS enrichment, processed samples were independently enriched with an overnight culture 100:1 (v/v) of any of the top five *Salmonella* serovars according to the Foodnet Canada Annual Report (Enteritidis, Newport, Heidelberg, Infantis, and Typhimurium) (PHAC 2017). Samples were then incubated overnight at 37°C. After incubation, bacteria were pelleted (10 000 × g for 5 min) and the supernatant was filtered using a 0.45-μm sy-

ringe filter. Dilutions of the filtrate were spotted onto a bacterial lawn of the respective *Salmonella* serovar used in that enrichment. For CE enrichment, overnight cultures of the top five *Salmonella* serovars mentioned above were mixed in equal ratios. Processed sample was added to the cocktail at a ratio of 100:1 (v/v) and incubated overnight at 37°C. Bacteria was pelleted as mentioned above and filtered using a 0.45-μm syringe filter. Dilutions of the filtrate were spotted onto a bacterial lawn of the respective *Salmonella* serovar. For CS enrichment, sample was mixed with 100 μl of an overnight of the first serovar of the series (e.g. *S.* Enteritidis) and incubated overnight at 37°C. Bacteria were pelleted and filtered as mentioned above. Dilutions of the filtrate were spotted onto a bacterial lawn of the same serovar and incubated overnight at 37°C to test for lytic activity. If lytic activity was observed, the filtrate was propagated in the same host (*S.* Enteritidis) by soft-agar overlay method as previously mentioned (Adams 1959). Subsequently, an overnight culture of the second serovar in the series (e.g. *S.* Newport) was diluted in fresh TSB media and incubated at 37°C until the culture reached mid-log phase ($OD_{600} = 0.1$). The culture was mixed with 100 μl of the phages that had first been propagated in *S.* Enteritidis and incubated overnight at 37°C followed by pelleting and filtration. Dilutions of the filtrate were spotted onto a bacterial lawn of the same serovar (*S.* Newport) and incubated overnight at 37°C to test for lytic activity against that serovar. If lytic activity was observed, the same procedure was followed as described above with the next serovar in the series. A serovar was omitted when no lytic activity was observed, and the series continued with the next serovar in line. For all three methods clear plaques were isolated by harvesting a single clear plaque on the respective host lawn using a sterile pipette tip. Plaques were suspended in 450 μl of CM (0.05 g/l gelatin; 6 ml/l 1 M Tris buffer; 0.735 g/l $CaCl_2$; pH 7.5) buffer, serially diluted and subjected to three passages on the respective host by double layer agar technique (Moreno Switt et al. 2013).

Phage propagation and cocktail preparation

Phage–host pairings used for propagation and experimental procedures are listed in Table S5 (Supporting Information). *Salmonella* phages were propagated as previously described (Moreno Switt et al. 2013) with some modifications. Briefly, liquid propagation was performed by mixing 100 μl of the respective *Salmonella* overnight culture with a single purified plaque. Mixture was incubated for 15 min at 37°C to allow phage adsorption followed by addition of 10 ml of TSB broth containing 2 mM $CaCl_2$ and overnight incubation at 37°C. Bacteria was pelleted and supernatant filtered through a 0.45-μm syringe filter to obtain crude lysates. Phage rfbG$_{rough}$ was propagated using solid propagation by mixing 100 μl of the respective *Salmonella* overnight culture with a single purified plaque. The mixture was incubated for 15 min at 37°C to allow phage adsorption followed by addition of 10 ml of molten (55°C) soft agar (TSB, 0.5% agar) broth containing 2 mM $CaCl_2$. The mixture was immediately poured onto TSA (1% agar) plates, let solidify, and incubated overnight at 37°C. The viral particles were harvested by adding 5 ml of CM to the agar surface and incubated for 4 h at room temperature. The liquid suspension was collected and filtered through a 0.45-μm syringe filter to obtain crude lysates. Lysates from both methods were stored at 4°C until further use. Each phage lysate was titrated by overlay method (Kropinski et al. 2009). Lysate was serially diluted in CM buffer, spotted onto respective host lawns, and incubated overnight at 37°C. Plaques were counted and reported

as PFU/ml. The phage cocktail was prepared by mixing the final selected individual phages at an equal ratio to a final titer of 9 log_{10} PFU/ml.

High throughput host range characterization in liquid culture

Host range was determined using a high throughput turbidimetric assay in a 384-well plate format (Corning, USA) as previously described (Martinez-Soto et al. 2021). A total of 20 NTS serovars listed in Table S2 (Supporting Information) were tested against all isolated phages. Phages were titrated and appropriately diluted to a final concentration of 7 log_{10} PFU/ml in CM buffer. *Salmonella* overnight cultures were diluted in 2X TSB to a final concentration of 7 log_{10} CFU/ml. Bacteria was mixed with phage in a total volume of 80 μl (40 μl of bacteria dilution + 40 μl of phage dilution) to a final Multiplicity of Infection (MOI) of 1 (bacteriophage/bacteria). The assay was performed using a 384-well plate, in which four phages against 22 serovars were tested per plate. Plate was incubated at 25°C for 24 h with continuous orbital agitation using a BioTek Synergy H1 Hybrid Multi-Mode Reader (Winooski, VT, USA). Optical density readings at wavelength of 600 nm were taken at 30 min intervals.

PHIDA: data analytics tool for efficient host range determination

Growth curves were analyzed using the Phage–Host Interaction Data Analyzer (PHIDA) (Martinez-Soto et al. 2021). The analysis is based on bacterial growth, specifically the time it takes to the untreated culture (phage free) to reach exponential growth phase ($OD_{600} = 0.2$ "detection threshold") compared to the phage treated control. A letter was designated based on the growth inhibition efficiency of the phage (s) treatment. C, complete inhibition of the bacterial growth; sample never reach detection threshold for the whole duration of the experiment. D+, more than 5 h delay in bacterial growth compared to control; time difference to reach detection threshold between sample and control is ≥ 5 h. D, less than 5 h delay in bacterial growth compared to control; time difference to reach detection threshold between sample and control is ≥ 1 and < 5 h. N/L, N/L+, or N/L++, 70%–85%, 40%–70%, and below 40%, respectively of the endpoint controls OD_{600} value. Phage clustering was performed using the Ward's minimum-variance method.

Receptor screening

Single gene mutants from the *Salmonella* Typhimurium ATCC14028 transposon library were used for identification of phage receptor on bacterial cell wall (Table S3, Supporting Information) (Santiviago et al. 2009). Bacteria were cultured in 5 ml of TSB media supplemented with the appropriate antibiotic (kanamycin 50 μg/ml or chloramphenicol 25 μg/ml) and incubated for 18 h at 37°C. Bacterial lawns were prepared and selected *Salmonella* phages were spotted in 10-fold serial dilutions. The receptor was determined based on the presence or absence of lysis area and individual plaques. The receptor for all selected phages in the cocktail was validated by complementation assays. Genes *ompC*, *btuB*, and *rfaL* were amplified using primers listed in Table S4 (Supporting Information) and cloned into pBAD24 and transformed into the respective *S.* Typhimurium mutants. Phages were spotted onto lawns of the transformed mutants supplemented with kanamycin 50 μg/ml and ampicillin 100 μg/ml. Receptor identification was confirmed based on the presence or absence of lysis area and individual plaques.

Bacteriophage insensitive mutant frequency and cross-resistance assays

The frequency of bacteriophage insensitive mutant (BIM) development was determined for individual, and cocktail of phages as previously described (El-Dougdoug et al. 2019). Individual phage or cocktail was mixed with the bacterial host *Salmonella* Enteritidis at a MOI of 100 (7 $\log_{10}$ CFU/ml bacteria and 9 $\log_{10}$ PFU/ml phages) and incubated for 20 min at 37°C to allow phage adsorption. Then, 5 ml of molten overlay agar were added and poured onto TSA plates. The plates were incubated for 24 h at 37°C. Colonies were counted, and the BIM frequency was calculated by dividing the number of surviving colonies by the number of bacteria added. A total of 10 bacteriophages resistant strains for every phage (except the rough specific phage rfbG$_{\text{rough}}$) were randomly selected from the growing BIMs and purified three times. A single colony was incubated in 10 ml of TSB media overnight for bacteria lawn preparation. Susceptibility to phage infection was reported as efficiency of plaquing (EOP). Strains with an EOP < 0.1 was reported as a resistant strain.

Transmission electron microscopy

The morphology of all five selected *Salmonella* phages was analyzed using Transmission electron microscopy (TEM.) To prepare the phages for TEM, 1 ml of phage stocks $\geq$ 9 $\log_{10}$ PFU/ml was centrifuged at 16 000 × *g* for 1 h at 4°C (Microfuge R centrifuge, Beckman Coulter Inc.) and washed twice with HEPES buffer (0.1 M, pH 7.4). Copper–rhodium (400-mesh) grids were covered with a thin layer of amorphous carbon made hydrophilic by 45 s vacuum glow-discharge. Phage solution samples (4–6 µl) were placed on individual grids and left for 2 min to adsorb onto the carbon. Excess sample was gently removed by touching filter paper to the edge of the droplet after adsorption was stablished. Excess small molecule contaminants were washed from the grid with three rinses of water. Sample on the grids were stained with 2% (w/v) uranyl acetate. A Tecnai G2 transmission electron microscope (FEI Company, Hillsboro, OR, USA) at Electron Microscopy Unit, University of Guelph (Guelph, ON, Canada) was used for visualization, operating at 200 kV under variable magnification (x 50 000). Images were acquired using the Gatan Ultascan 4 K CCD (Pleasanton, CA, USA) and Gatan Digital Micrograph software imaging system.

Phage adsorption kinetics and one-step growth curves

Phage adsorption experiment was performed as described previously (Kropinski 2009). Briefly, *Salmonella* overnight cultures were diluted 1/50 (~OD600 = 0.04) in TSB supplemented with 2 mM CaCl$_2$ and incubated until an OD$_{600}$ = 1 was reached (8 log10 CFU/ml). Bacteriophage was added to a final concentration of 5 $\log_{10}$ PFU/ml (MOI = 0.001). Mixtures were incubated for 15 min at 37°C with moderate agitation. Samples were taken at 3 min intervals and immediately added to TSB aliquots containing three drops of chloroform (CHCl$_3$). Viral titers were determined by double-layer plaque assay using susceptible *Salmonella* as a host. Adsorption was reported as percentage of free phage by normalizing with initial titer.

Phage one-step growth curve (OSGC) were performed as described previously with some modifications (Park et al. 2012). Bacterial cultures corresponding to phage amplification hosts were grown overnight in TSB at 37°C with shaking at 200 rpm. A volume of 1 ml of bacterial culture was then transferred to 9 ml of TSB and incubated (37°C, 170 rpm) until an OD600 of 0.5 was ob-

served (~8 log10 CFU/ml). Phages were added to their corresponding bacterial culture at MOI = 0.01 and incubated for 3–8 min (based on adsorption rate) at 37°C to allow phage adsorption. Immediately after adsorption, 100 µl of the mixture were diluted in 9.9 ml (1/100 dilution, 1/1000 for rapidly adsorbing phage CE$_{\text{LPS}}$) of fresh TSB media tempered at 37°C to avoid further phage adsorption. Phage–bacteria dilution was incubated at 37°C for 1 h, with aliquots taken every 5 min. Aliquots were immediately serial diluted in CM buffer and titrated. The spotted plates were incubated at 37°C overnight for plaque counting and visualization. Burst size was calculated using the following formula: Burst size = (Final titer−Initial Titer)/(Initial titer).

Effect of phage cocktail concentration on the growth of NTS Strains in liquid culture

A total of 66 NTS strains (representing 20 serovars) (Tables S1 and S2, Supporting Information) were tested against a phage cocktail comprised of five selected phages. Individual bacteriophages were titrated and mixed in equal ratios and diluted in CM buffer to a final concentration of 6–9 $\log_{10}$ PFU/ml. Overnight cultures were diluted in 2X TSB to a final concentration of 6 $\log_{10}$ CFU/ml. Bacteria were mixed with phage in a total volume of 80 µl (40 µl of bacteria dilution + 40 µl of different concentrations of phage cocktail) to achieve MOI of 1, 10^1, 10^2, and 10^3. The assay was performed using a 384-well plate with three technical replicates per MOI. Plate was incubated at 25°C for 24 h with continuous orbital agitation using a BioTek Synergy H1 Hybrid Multi-Mode Reader. Readings at 600 nm wavelength were taken every 30 min.

Phage genome extraction and sequencing

High titer phage suspensions were treated with DNase I (4 µg/ml) and RNase A (2 µg/ml) and incubated at 37°C for 20 min followed by thermal inactivation at 75°C for 10 min. Nucleic acid extraction was performed using Invitrogen's PureLink™ Viral RNA/DNA mini kit (Invitrogen, Waltham, Massachusetts, USA) following manufacturer's instructions. The nucleic acid samples with variable concentrations from ranging from 17 to 628 ng/µl were mechanically sheared to 550 bp insert using Covaris M220 instrument (Covaris, USA). The obtained inserts were used as a template to construct PCR free Libraries with NxSeq AmpFREE Low DNA Library kit (Lucigen) according to the manufacturer's instructions. Single indexed libraries were pooled, and sequencing was carried out on a MiSeq instrument (Illumina) using 2 × 300 bp MiSeq Reagent Kit v3 600 Cycles (Illumina) according to the manufactures recommendations in order to obtain the paired-end reads. The raw sequencing reads for all *Salmonella* phages were submitted to NCBI sequence read archive under the BioProject ID: PRJNA1058572

Genome assembly

Two different pipelines were used for assembly of the phage genomes. Genome assembly of phage CE$_{\text{LPS}}$ was performed using Geneious prime (https://www.geneious.com/). Briefly, Paired-end reads were trimmed for quality control using BBTools package BBDuk adapter/quality trimmer (version 38.84), short reads of < 50 bp were discarded and minimum quality control was set to 20. Trimmed reads were normalized by target coverage and depth using BBNorm error correction and read normalization tool (version 38.84). Trimmed and normalized reads were assembled using SPAdes (version 3.13.0) (Bankevich et al. 2012). For the assembly of phages NP4$_{\text{OmpC}}$, ECS$_{\text{BtuB}}$, and ssTn$_{\text{LPS}}$ were processed using bioinformatics software DNASTAR (https://www.dnastar.com/) and as-

sembled using SeqMan NGen15 (DNASTAR, Madison, WI, USA) algorithm.

Structural and functional annotation of phage genomes

All *Salmonella* phage genomes were structurally and functionally annotated using Galaxy CPT Apollo (Ramsey et al. 2020). Complete annotation was performed using the "PAP Structural Workflow v2021.02" and "PAP Functional Workflow v2022.01". Briefly, CDS were called using MetaGeneAnnotator, Glimmer3, and Sixpack. Ribosome binding sites, rho-independent terminators, and tRNAs were called using Shine Find, TransTermHP, and tRNAscan-SE, respectively. The putative function of genes was inferred by nucleotide and protein BLAST [64]. Domains and other predictions were called using InterProScan, TMHMM, SignalIP, and LipoP SPII. The annotated genomes of CE_{LPS} (vB_SenS-AKM_CE), ECS_{BtuB} (vB_SenS-AKM_ECS), $NP4_{OmpC}$ (vB_SenM-AKM_NP4), and $ssTn_{LPS}$ (vB_SenM-AKM_ssTn) were submitted to the NCBI nucleotide database under the accession numbers OR122686, OR122687, OR122689, and OR122688, respectively.

Presence of lysogeny, antimicrobial resistance, and virulence genes

All predicted CDS were manually analyzed for the presence of integrases. Additionally, phage CDS were analyzed using the Phage Classification Tool Set (PHACTS) (McNair et al. 2012). PHACTS utilizes a novel similarity algorithm and a supervised Random Forest classifier to make a prediction as to whether the lifestyle of a phage, described by its proteome, is virulent or temperate. Scores of the newly sequenced phages were compared to well characterized lytic (Felix 01, NC_005282.1) and temperate (P22, NC_002371.2) *Salmonella* phages. Screening for the presence of antimicrobial genes was performed on the Comprehensive Antibiotic Resistance Database (CARD) using the Resistance Gene Identifier (RGI; McArthur et al. 2013). Additionally, phage proteomes were analyzed using the Virulence Factor Data Base (VFDB) to find potential virulence factors encoded in the phage genomes (Liu et al. 2019).

Phage phylogenetic trees

Phage phylogenetic trees were generated using whole genome sequences CDS and the large terminase subunit. Trees derived from whole genome sequences CDS were created using the ViP-Tree (https://www.genome.jp/viptree/) algorithm and the RefSeq phage data base (Nishimura et al. 2017). Large terminase subunit tree was generated using the Neighbor-joining algorithm in Geneious Prime (https://www.geneious.com/) with sequences downloaded from the RefSeq phage data base (McGinnis and Madden 2004).

Biocontrol experiment on chicken skin

Chicken skin samples were extracted from chicken carcasses obtained from local grocery stores. Using kitchen shears, the skin was carefully cut into 1 cm^2 pieces. Chicken skin pieces were placed in 12-well plates and covered to avoid complete desiccation. Chicken skin pieces (*n* = 3) were mixed with 1 ml of PBS buffer and plated XLT-4 plates to assess for background *Salmonella* contamination. Chicken skin was inoculated by adding 50 µl of bacterial suspension in PBS (5 log_{10} CFU/ml) and spread evenly on the skin surface to a final bacteria concentration was 4 log_{10} CFU/cm^2. Following inoculation, all pieces were dried to allow bacteria attachment in a biological safety cabinet for 20 min. The

phage cocktail with equal ratios of each phage was adjusted in CM buffer to two final concentrations of 5 and 7 log_{10} PFU/ml. Phage treatment was performed by adding 1 ml of phage suspension into the wells. Plates were incubated at room temperature for 10 min to allow phage attachment to the food matrix. Immediately after incubation, the excess phage solution was drained from the wells. Plates were covered in parafilm to avoid desiccation and incubated at 4°C, 15°C, and 25°C. At the indicated time points (30 min, 1, 6, 12, 24, 48, and 72 h) samples were placed in 2 ml microfuge tubes containing 1 ml of sterile PBS buffer. Tubes were vortexed for 120 s to allow detachment of bacterial cells. Before plating, 100 µl of the homogenate were mixed with 100 µl of virucide solution and incubated 10 min at RT to remove residual phage (Chibeu and Balamurugan 2018). Dilutions were performed and samples were plated on XLT-4 (Difco™) followed by incubation at 37°C overnight. Each treatment was performed in three replicates. Colonies were counted and reported as CFU/cm^2.

Genome-wide transduction frequency calculation

The phage transduction frequency was calculated in a genome-wide manner using a 230 K complexity S. Typhimurium Tn5 Kanamycin library (Moraes et al. 2017, Fitzsimmons et al. 2018). All phages (except the rough specific phage $rfbG_{rough}$) were propagated in exponentially growing S. Typhimurium T5 library cultures as indicated in section 2.4. All phages were amplified for a minimum of 1.5 log_{10} PFU/ml to ensure > 95% phage progeny was propagated in the library. Phage progenies were used for classical transduction assays as previously described. Briefly, recipient strain S. Typhimurium ATCC14028 was grown overnight at 37°C followed by dilution to an 8 log_{10} CFU/ml in TSB with 2 mM $CaCl_2$. Cells were infected with 7 log_{10} PFU/ml and incubated for sufficient time to allow > 90% adsorption. To prevent reinfections, unbound phages were removed by centrifugation. Cells were resuspended in 1 ml of TSB + 200 µl of 1 M sodium citrate and allowed to recover at 37°C for 30 min. Cells were pelleted, resuspended in 100 µl TSB and plated on TSA plates supplemented with kanamycin 50 µg/ml.

Statistical analysis

Phage host range screening was performed in triplicates and compared to the vehicle control are previously reported (Martinez-Soto et al. 2021). The statistical significance of phage BIM frequency, receptor complementation, and transduction experiments were confirmed at the 5% level using a one-way analysis of variance (ANOVA) followed by Duncan's multiple range tests.

Biocontrol experiment statistical analyses were performed by ANOVA followed by Tukey's test with 95% confidence interval. All statistical analysis was done using Prism 8.01 for Windows (GraphPad software, San Diego, CA, USA).

Results

Isolation and host range pattern/profile of isolated *Salmonella* phages

A total of 40 *Salmonella* phages were isolated from various samples, including sewage plant wastewater, retail chicken skin, chicken feathers, and river water. Phages were isolated using three sample enrichment methods: (1) single serovar enrichment, (2) cocktail enrichment, and (3) CS enrichment as previously reported

(Martinez-Soto et al. 2021). The host range of the phage isolates was determined using 22 strains from 20 NTS serovars (Table S2, Supporting Information). A total of 11 phage clusters were identified based on the host range profiles (Cluster A–K) (Fig. 1). Both, narrow (e.g. cluster K) and broad host range phage (e.g. cluster A) clusters were found. Moreover, a significant majority of the isolates (33/40) inhibited the growth of S. Enteritidis, a serovar used in all the enrichment methods. This screening technique allows for the selection of broad host range phages and the discrimination of potential phage reisolates. For instance, phages in the same cluster have a highly similar host range, suggesting the reisolation of closely related phages. With the exception of clusters, I, J, and K, representative phages from each cluster were selected for receptor identification as these phages were deemed as broad host range based on number of hosts used.

Receptor screening and complementation

As the final goal of the isolation/screening is to select broad host lytic phages with distinct characteristics, 19 phages representing clusters A–H (Fig. 1 and Table 1) were selected for receptor screening using S. Typhimurium single gene receptor knockouts (Table S3, Supporting Information). A total of five (5/19) phages could not infect the strain S. Typhimurium $\Delta rfbG$ or $\Delta rfaL$, these genes encode for enzymes involved in the biosynthesis pathway of the O-antigen in *Salmonella* (MacLachlan et al. 1991, Calva et al. 2015). Thus, suggesting these phages are likely to use the O-antigen as receptor. Six phages (6/19) showed to require the vitamin B transporter BtuB as a receptor, reflected in no infection to the mutant strain S. Typhimurium $\Delta btuB$. Moreover, four (4/19) phages showed no infection on S. Typhimurium $\Delta ompC$, suggesting the usage of this protein as receptor (Table 1). Interestingly, a positive correlation between the host range profile clustering and receptor recognition was observed. For instance, all phages in cluster A and cluster H required OmpC and O-antigen as receptors, respectively. Furthermore, 2/3 phages in clusters C and E utilized BtuB as receptor. Phage SP24 and SP38 could not infect the parental strain S. Typhimurium, therefore, their receptor was reported as unknown. Phage SP26 and SP37 showed productive infection in the parental strain but no lysis zone or plaques were observed in any receptor mutants. Their receptor was reported as inconclusive in this experiment.

Taking into consideration these results, four phages were selected for assembly into a cocktail based on: (1) host range profile, (2) receptor recognition, and (3) large-scale propagation feasibility (routinely obtained titres $\geq$ 10 $\log_{10}$ PFU/ml). Phages SP04, SP19, SP33, and SP07 were selected based on these features. They were subsequently renamed as vB_SenM-AKM_NP4, vB_SenS-AKM_CE, vB_SenS-AKM_ECS, and vB_SenM-AKM_ssTn, now referred to as NP4$_{OmpC}$, CE$_{LPS}$, ECS$_{BtuB}$, and ssTn$_{LPS}$, respectively. The cocktail includes phages that target three different receptors: (1) O-antigen (CE$_{LPS}$ and ssTn$_{LPS}$), (2) BtuB (ECS$_{BtuB}$), and (3) OmpC (NP4$_{OmpC}$).

Gene complementation assays were performed in the *Salmonella* Typhimurium receptor mutant strains to validate the phage utilization (Fig. 2). Genes *rfaL* (O-antigen ligase), *btuB*, and *ompC* were cloned into the expression vector pBAD24 and transformed into the respective receptor knockouts. In all but one case, phage infection was restored in the complemented strains to the same EOP levels as the WT strain. The only exception was phage CE$_{LPS}$, where the EOP in the complemented mutant was 0.35, suggesting that the expression level of *rfaL* in the complementing plasmid was suboptimal to restore full WT O-antigen functionality.

Quantification of resistance emergence and cross-resistance assays

The frequency of BIM emergence was assessed for all phages individually. *Salmonella enterica* subsp. *enterica* serovar Enteritidis was selected for this assay, as this serovar is responsible for 43% of the food-borne salmonellosis cases in Canada (PHAC 2017). The O-antigen-dependent phage CE$_{LPS}$ showed the lowest BIM frequency of 3.93×10^{-5}. The remaining phages exhibited a higher BIM frequency against S. Enteritidis (Fig. 3A). S. Enteritidis can generate BIMs completely resistant to CE$_{LPS}$ and ssTn$_{LPS}$ (Table S6, Supporting Information; Fig. 3B). Since these phages use the O-antigen as a receptor, a mutation that either modifies or truncates the production of O-antigen will exhibit resistance. For this reason, a screen was performed to isolate O-antigen-independent phages using the O-antigen deficient mutant strains S. Typhimurium $\Delta rfbG$ and $\Delta rfaL$. A new phage named rfbG$_{rough}$ was isolated; this phage showed strong lytic activity against S. Typhimurium $\Delta rfbG$ and $\Delta rfaL$ but no infection against the parental strain with intact O-antigen. Complementation of the $\Delta rfaL$ receptor mutant blocked the infection of rfbG$_{rough}$ (Fig. 2). This suggests that rfbG$_{rough}$ is a rough specific phage (Kim et al. 2014).

Randomly selected BIMs isolated from the O-antigen dependent phages CE$_{LPS}$ and ssTn$_{LPS}$ were susceptible to the infection of rfbG$_{rough}$ with an EOP of 1 (Table S6, Supporting Information; Fig. 3B). These results indicate that O-antigen-dependent phages in the cocktail can select for BIMs with modified O-antigen. The rough specific phage can then infect these mutants in a layered cocktail manner (Hesse et al. 2020). Inclusion of the rough specific phage significantly reduced the BIM frequency of the cocktail >10-fold–6.22×10^{-6}, significantly lower compared to single phage CE$_{LPS}$ ($P = .0095$) (Fig. 3A). To better understand the resistance emergence, 10 BIMs were isolated from single phage treatment ($n = 40$) and an EOP assay was performed with all phages in the cocktail. As shown in Fig. 3(B), most BIMs were susceptible to the infection of at least one of the phages in the cocktail. No BIMs isolated from a single phage were cross-resistant to all the phages. This can explain the high effectiveness of the phage cocktail compared to a single phage treatment. Moreover, over half of the BIMs isolated from the O-antigen-dependent phages (CE$_{LPS}$ and ssTn$_{LPS}$) were resistant to rfbG$_{rough}$. This resistance can be nonreceptor related, leading to smooth BIMs with complete O-antigen that are resistant to phages CE$_{LPS}$, ssTn$_{LPS}$, and rfbG$_{rough}$.

Combined efficacy of the multireceptor phage cocktail

The effectiveness of bacterial lysis was further evaluated in an *in vitro* turbidimetric assay. A total of 10 biological replicates, each performed in six technical replicates ($n = 60$) of S. Enteritidis were infected with the phage cocktail at an MOI of 5. The growth kinetics were evaluated for 72 h to identify the regrowth of resistant mutants. Out of 60 replicates, the phage cocktail completely inhibited the growth of 38, while the remaining 22 showed poor growth and reduced growth compared to the control (Fig. 3C). Lastly, the phage inhibition efficacy was evaluated *in vitro* at 15°C to simulate improper storage temperature of poultry products (Yimenu et al. 2019). The phage cocktail completely inhibited the growth of S. Enteritidis for up to 120 h (Fig. 3D). Together, these results demonstrate that the systematic cocktail design can significantly reduce the emergence of resistance, prevent cross-
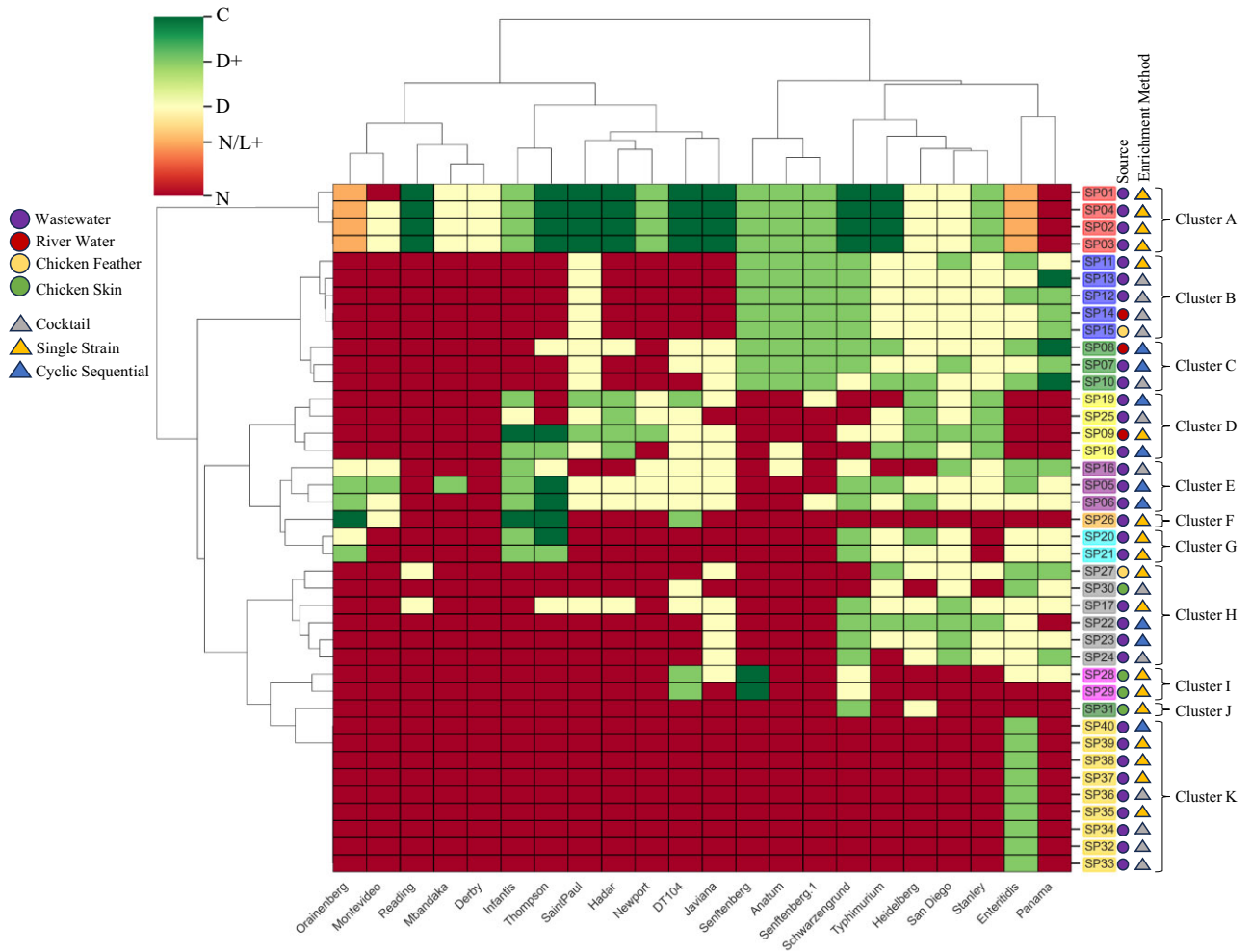
Figure 1. Host range clustered heat map of *Salmonella* phages. Salmonella strains were infected with phage at MOI of 1 and incubated at 25 °C for 24 h in TSB. Growth inhibition designation: C: complete inhibition. D+: >5 h delay to reach exponential phase. D: <5 h delay to reach exponential phase. N/L+: <70% ODmax. N: no effect. Clustering was performed using the Ward's minimum-variance method.

**Table 1.** Receptor screening of isolated *Salmonella* phages.

Strain/phage	Host range cluster	ParentalATCC14028 strain	ΔbtuB	ΔfhuA	ΔfliR	ΔompC	ΔompA	ΔrfaL	ΔrfbG	Putative receptor
SP01	A	(+), P	(+), P	(+), P	(+), P	(−), NP	(+), P	(+), P	(+), P	OmpC
SP02	A	(+), P	(+), P	(+), P	(+), P	(−), NP	(+), P	(+), P	(+), P	OmpC
SP03	A	(+), P	(+), P	(+), P	(+), P	(−), NP	(+), P	(+), P	(+), P	OmpC
SP04	A	(+), P	(+), P	(+), P	(+), P	(−), NP	(+), P	(+), P	(+), P	OmpC
SP20	B	(+), P	(−), NP	(+), P	(+), P	(+), P	(+), NP	(+), P	(+), P	BtuB
SP19	C	(+), P	(+), P	(+), P	(+), P	(+), P	(+), P	(−), NP	(−), NP	O-antigen
SP35	C	(+), P	(−), NP	(+), P	(+), P	(+), P	(+), P	(+), P	(−), NP	BtuB
SP36	C	(+), P	(−), NP	(+), P	(+), P	(+), P	(+), P	(+), P	(+), NP	BtuB
SP05	D	(+), P	(+), NP	(+), NP	(+), NP	(+), NP	(+), NP	(−), NP	(−), NP	O-antigen
SP26	D	(+), P	(−), NP	(−), NP	(−), NP	(−), NP	(−), NP	(−), NP	(−), NP	Inconclusive
SP37	D	(+), P	(−), NP	(−), NP	(−), NP	(−), NP	(−), NP	(−), NP	(+), NP	Inconclusive
SP38	D	(+), NP	(−), NP	(−), NP	(−), NP	(−), NP	(−), NP	(−), NP	(−), NP	Unknown
SP24	E	(−), NP	(+), NP	(+), NP	(+), NP	(+), NP	(+), NP	(+), NP	(+), NP	Unknown
SP33	E	(+), P	(−), NP	(+), P	(+), P	(+), P	(+), P	(+), P	(−), NP	BtuB
SP34	E	(+), P	(−), NP	(+), P	(+), P	(+), P	(+), P	(+), P	(+), P	BtuB
SP08	G	(+), P	(−), NP	(+), P	(+), P	(+), P	(+), P	(+), P	(+), P	BtuB
SP07	H	(+), P	(+), P	(+), P	(+), P	(+), P	(+), P	(−), NP	(−), NP	O-antigen
SP39	H	(+), P	(+), P	(+), P	(+), P	(+), P	(+), P	(−), NP	(−), NP	O-antigen
SP40	H	(+), P	(+), P	(+), P	(+), P	(+), P	(+), P	(−), NP	(−), NP	O-antigen

(+): lysis zone, (−): no lysis zone, P: individual plaques, and NP: no individual plaques.
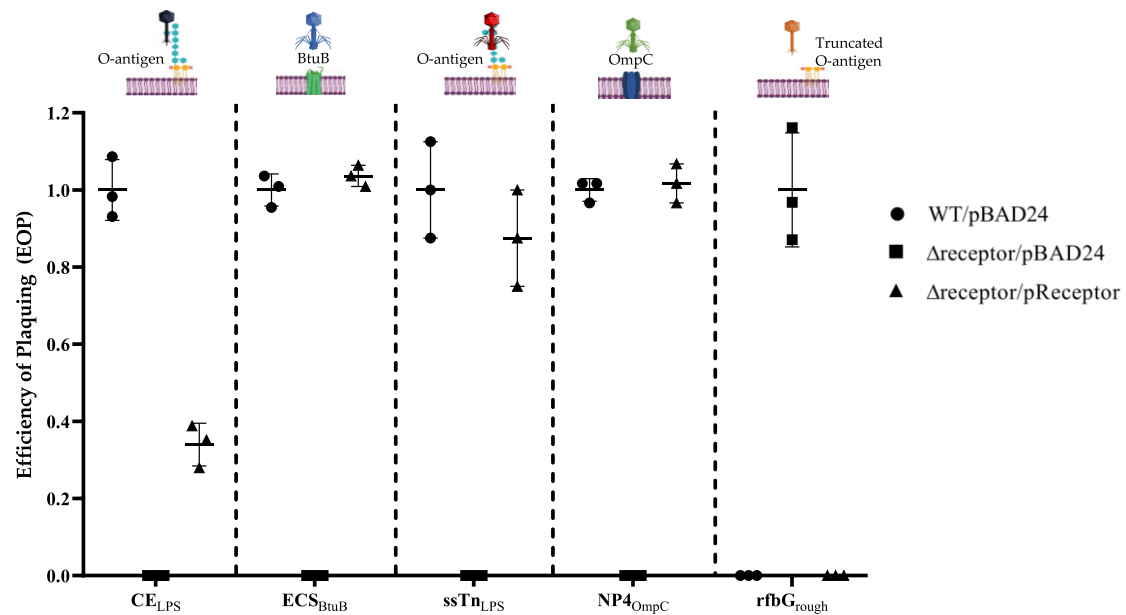
Figure 2. EOP of four selected *Salmonella* phages on the respective receptor knockouts and genecomplemented strains. EOP receptor complementation assay of selected Salmonella phages. Receptor genes were cloned into a pBAD24 vector. O-antigen (prfaL), BtuB (pbtuB), and OmpC (pompC). Data shown as means ± SD of three replicates.
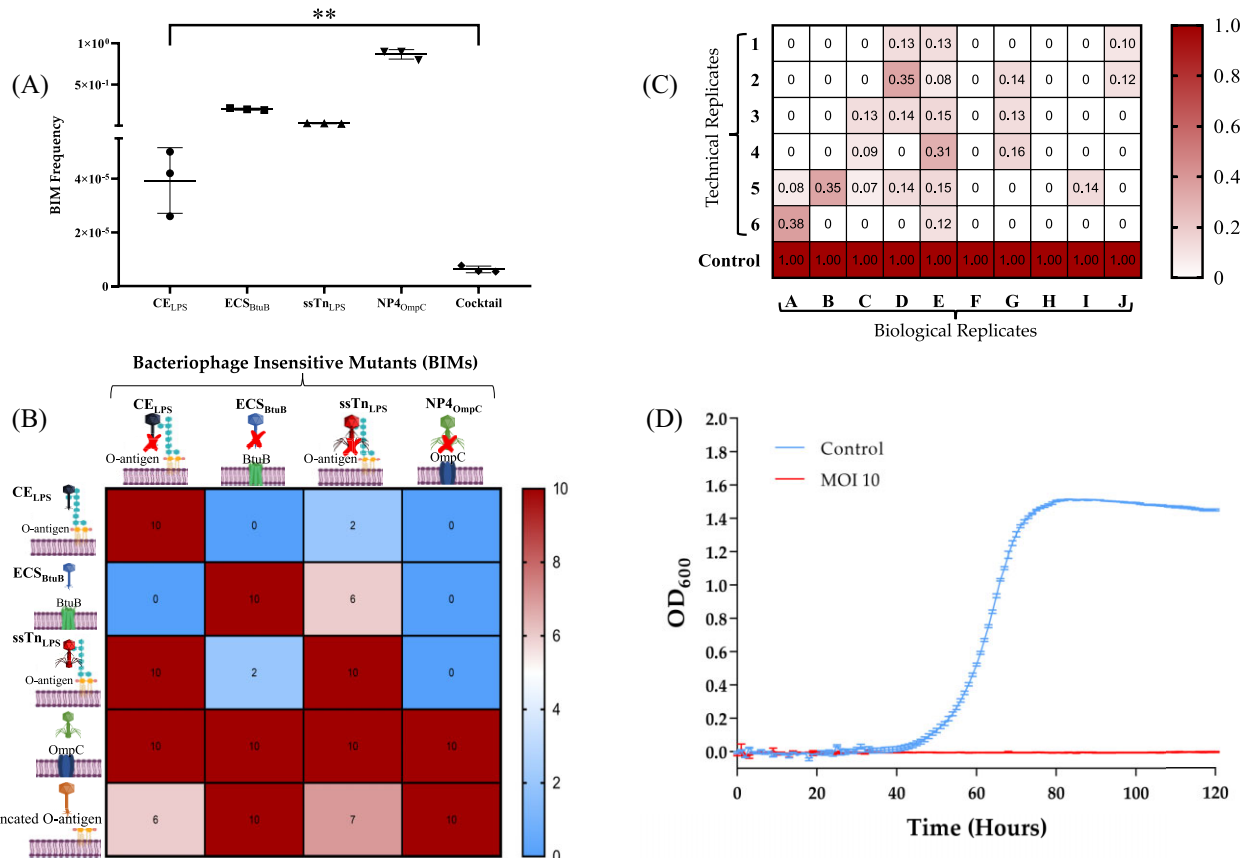
Figure 3. Emergence of phage resistance in S. Enteritidis. (A) BIM frequency against individual phage and phage cocktail. (B) Heat map of Bacteriophage cross-resistance assay. Susceptibility to phage infection was assessed by EOP. Phage resistance was reported when EOP < 0.1. (C) Bacterial cultures were challenged with the cocktail at an MOI of 5 and incubated at 25°C for 72 h in TSB. Numbers indicate the growth rate normalized to the control. (D) Bacteria challenge experiment at 15°C. Cultures were treated with phage at MOI of 10 and growth kinetics was evaluated for 120 h using a turbidimetric assay.

resistance, and inhibit the growth of *Salmonella* for prolonged periods.

Phage morphology and infection kinetics

Four of the five phages included in the cocktail were imaged by TEM and identified as tailed phages (Fig. 4B). CE_{LPS} and ECS_{BtuB} both showed an icosahedral head and a long noncontractile tail characteristic of the siphovirus morphotype. Conversely, phage $NP4_{OmpC}$ and $ssTn_{LPS}$ exhibited an icosahedral capsid and a long contractile tail, a morphotype expected of a myovirus. Contrary to the other phages, $rfbG_{rough}$ displayed isometric capsids of 60 nm diameter with no visible tails. This morphology has been described previously in phages belonging to the *Corticoviriade* and *Tectiviridae* family (Oksanen and Ictv Report 2017, Caruso et al. 2019). The stability of these phages was evaluated across various environmental conditions. Notably, all phages exhibited robust stability at 60°C for 60 min, with CE_{LPS} and ECS_{BtuB} demonstrating remarkable heat resistance at 70°C. Additionally, the phages demonstrated resilience across a wide pH range (pH 4–11), with variations in stability observed at extreme pH values (Figure S1, Supporting Information).

The infection kinetics for all phages were evaluated. All phages showed rapid adsorption to their respective hosts (Figure S2, Supporting Information), with adsorption constants ranging from 7.5×10^{-10} to 2.55×10^{-9} PFU/ml/min (Fig. 4C). The latent period ranged from 10 to 25 min with variable burst sizes of 15–139 (Figure S3, Supporting Information) (Fig. 4C). The morphotypes and infection kinetics of the phage strongly suggest that they differ from each other and relate to the complementarity of their performance in infection and low levels of cross-resistance.

Effect of phage cocktail concentration on the growth of NTS strains in liquid culture

A total of 66 *Salmonella* strains representing 20 serovars were used for this assay. These include the 20 NTS strains that were used for host range screening and 44 additional strains listed in Table S1 (Supporting Information) and Table S2 (Supporting Information), respectively. Multiple strains were screened from each serovar: Enteritidis (eight strains), Typhimurium (nine strains), Kentucky (nine strains), Newport (six strains), Heidelberg (six strains), and Saint Paul (six strains). All hosts were adjusted to a final concentration of 6 $\log_{10}$ CFU/ml and infected with the phage cocktail at MOI of 1–1000 (6–9 $\log_{10}$ PFU/ml). At the highest phage concentration (MOI of 1000, 9 $\log_{10}$ PFU/ml), the phage cocktail inhibited the growth (different degrees of inhibition) of all *Salmonella* strains tested (Fig. 5). The number of strains and serovars inhibited increased in a concentration-dependent manner. This demonstrates that the phage cocktail formulated in this study is a promising biocontrol tool to mitigate contamination and prevent the growth of all these strains.

Genome analysis and identification of genes encoding for receptor binding proteins

The whole genomes of CE_{LPS}, ECS_{BtuB}, $NP4_{OmpC}$, and $ssTn_{LPS}$ were sequenced and annotated. All phages possess linear dsDNA genomes ranging from 41 337–159 291 bp with a %GC of 33.9%–50.0% (Table 2). As expected, based on the phenotypic characterization, these phages belong to distinct subfamilies/families: *Guernseyvirinae*, *Tevenvirinae*, *Demerecviridae*, and *Ackermannviridae* (Table 2). Using the Galaxy-Apollo platform, 25%–45% of the genes encoded in the genomes were functionally annotated

(Tables S7–S10, Supporting Information). Genes encoding for tR-NAs were also found in the phages $NP4_{OmpC}$, ECS_{BtuB}, and $ssTn_{LPS}$ (Table 2).

Functional genes encoding proteins involved in receptor recognition were identified in the phage genomes (Tables S7–S10, Supporting Information). *AKMCE_029–30* and *AKMssTn_001–2* were identified as genes encoding for potential receptor-binding proteins in the LPS-dependent phages CE_{LPS} and $ssTn_{LPS}$, respectively. *AKMCE_029–30* encode for tail spikes, a multiprotein recognition device that facilitates the recognition of protein or carbohydrate receptors in siphoviruses (Goulet et al. 2020). These gene products showed high identity to proteins with endorhamnosidase activity that can hydrolyze the O-polysaccharide chain in Gram-negative bacteria (Wollin et al. 1981). *AKMssTn_001–2* and *AKMssTn_115* encode tail spike and tail fibre proteins in phage $ssTn_{LPS}$, respectively. Both structures have been described as receptor-binding proteins recognizing the LPS of Gram-negative bacteria in myoviruses (Walter et al. 2008, Efimov et al. 2022). Moreover, *AKMssTn_072* gene product was identified as a tail-associated lysozyme in phage $ssTn_{LPS}$. In phage T5, the tail-associated lysozyme (Gp5) functions as a cell puncturing device and digests the peptidoglycan in the periplasmic space allowing the successful injection of the viral DNA (Kanamaru et al. 2005). Five genes (*AKMNP4_244–248*) were predicted encode for a multiprotein complex known as long tail fibers (LTF) in the OmpC-dependent phage $NP4_{OmpC}$ (Dunne et al. 2018). *AKMNP4_244–248* encode the LTF proximal subunit, hinge connector of the LTF, LTF distal hinge, large distal tail fiber subunit, and the receptor binding protein, respectively. All the gene products shared 100% identity and coverage with the genes forming the LTF (*gp34–38*) in *Salmonella* phage S16 infecting via the OmpC and LPS (Marti et al. 2013). Conversely, only one gene was predicted as a receptor-binding protein in the BtuB-dependent phage ECS_{BtuB}. *AKMECS_006* shares a high identity with the receptor-binding proteins encoded in T5-like phages belonging to the *Demerecviridae* family. Members of these families have also been reported as BtuB-dependent phages in *Salmonella*, and *Escherichia* (Kim and Ryu 2011, Bai et al. 2019, Liu et al. 2022). These findings are consistent with the experimental evidence of the receptor recognition of these phages (Table 2 and Fig. 2).

Presence of AMR and virulence factors

The amino acid sequence of all predicted coding sequences (CDS) encoded in the sequenced phages was submitted to the CARD and the VFDB (Table 2). No hits were identified in the CARD when using the RGI, meaning no previously identified AMR genes were present in the phage genomes. Additionally, the VFDB did not detect any proteins with high similarity to previously reported virulence factors. These results demonstrate that selected phages in this project are safe to use as biocontrol agents as no AMR or virulence factor is encoded in their genomes.

Phage replication cycle

Phages that undergo the lysogenic cycle are generally undesirable for phage therapy and biocontrol. These phages can encode for potential virulence factors and transduce bacteria with AMR genes favoring bacterial survival. For these reasons, phage genomes were manually parsed to identify the presence of integrase. Additionally, the lifestyle (replication cycle) of all sequenced phages was predicted using the Phage Classification Tool Set (PHACTS). Integrase genes were not identified in any of the genomes according to RAST and PHASTER databases. In contrast, an integrase
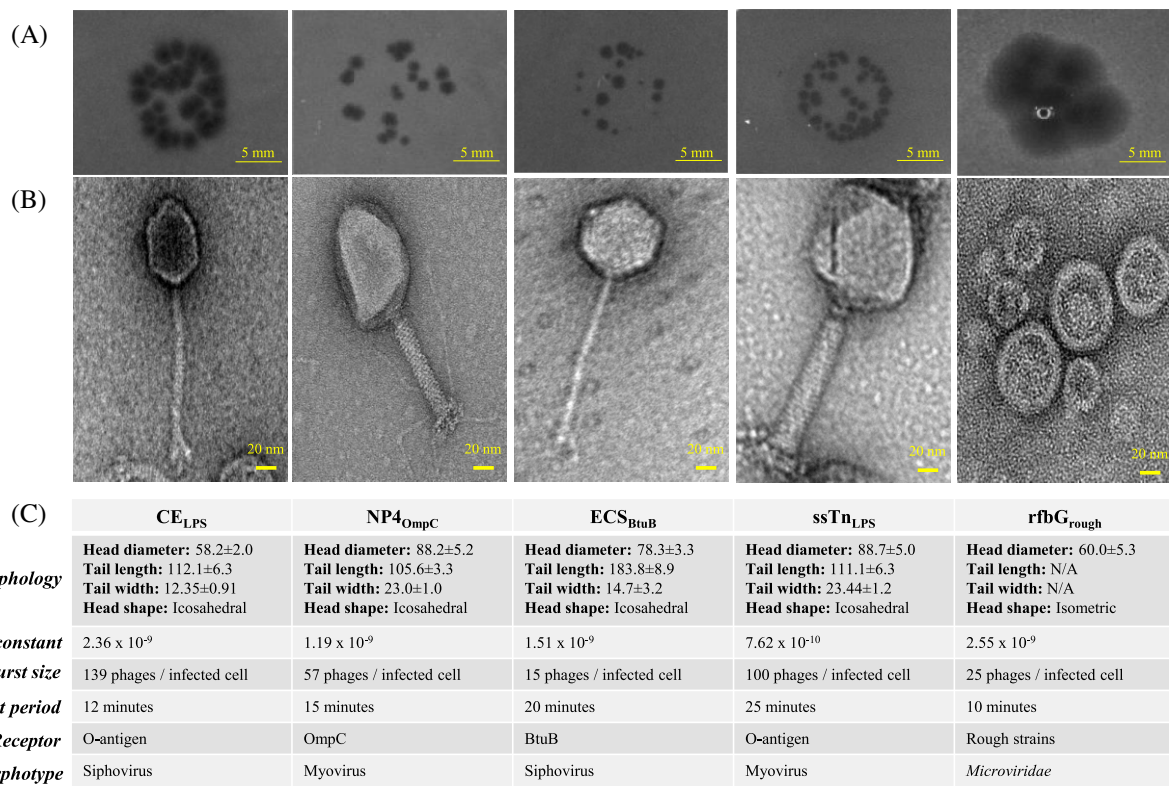
Figure 4. *Salmonella* phages selected for cocktail composition. (A) Plaques on the respective propagation hosts (Table S5). (B) Transmission electron micrographs. (C) Table of phage features.

Table 2. Genomic features of selected *Salmonella* phages.

	CE$_{LPS}$	NP4$_{OmpC}$	ECS$_{BtuB}$	ssTn$_{LPS}$	Felix O1(Whichard et al. 2010)	P22[a](Vander Byl and Kropinski 2000)
Size (bp)	41 337	159 273	114 722	159 291	86 155	41 27
%GC	50.0	36.9	40.3	44.9	39.0	47.1
CDS (#)	61	259	182	144	127	68
Genes[b] (#)	23	119	47	65	25	60
tRNA(#)	0	3	29	6	18	0
Family/subfamiliy/genus	*Guernseyvirinae*	*Tevenvirinae*	*Demerecviridae*	*Ackermannviridae*	*Ounavirinae*	*Lederbergvirus*
Virulence factors[c]	No	No	No	No	No	No
AMR genes[d]	No	No	No	No	No	No
Lytic score	0.503	0.558	0.509	0.549	0.594	0.277
Temperate score	0.497	0.442	0.491	0.451	0.406	0.723
Integrase	No	No	No	No	No	Yes

[a]Control phage; [b]genes with functional annotation; [c]Virulence Factor Data Base (VFDB); [d]Comprehensive Antimicrobial Resistance Data Base (CARD); [e]Phage Classification Tool Set (PHACTS); [f]Using PHASTER and RAST.

was identified in the control temperate phage P22 with RAST and PHASTER (Table 2). All phages exhibited a lytic score higher than the temperate score according to PHACTS, and all had scores similar to the lytic phage Felix O1. These results suggest that all the selected *Salmonella* phages in the cocktail are lytic.

Phage phylogeny

Two phylogenetic trees were generated using all predicted CDS (Fig. 6A) and the amino acid sequence of the large terminase subunit (Fig. 6B). As shown in Fig. 6(A), the selected *Salmonella* phages are located in unique clades compared to those deposited in the RefSeq phage database (Nishimura et al. 2017). The same trend is observed in the phylogenetic tree generated with the large ter-

minase subunit (Fig. 6B). Based on the sequence of this conserved protein, the phages are located in widely divergent clades. This demonstrates that the phage selection criteria implemented in this study can yield genetically distinct phages with unique genomic traits that can potentially benefit the efficacy of the cocktail.

Phage biocontrol experiment on chicken skin

The phage cocktail biocontrol efficacy was evaluated on chicken skin artificially inoculated with 4 log$_{10}$ CFU/cm^2 of *Salmonella*. The phage cocktail treatment significantly reduced bacterial loads at all time points and temperatures tested. A total of 30 min after phage treatment with 7 log$_{10}$ PFU/ml, a 1 log10 CFU/cm^2 reduc-
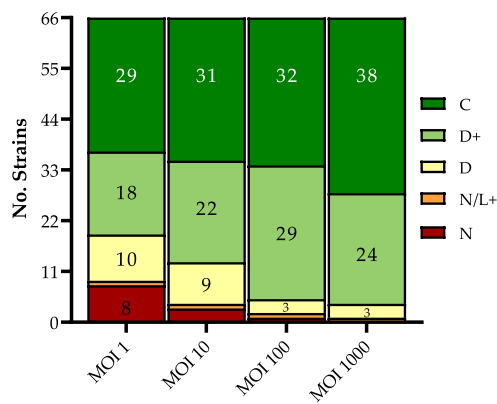
Figure 5. Bacteriophage cocktail growth inhibition against 66 S. enterica strains. 6 log10 CFU/mL were treated with phage at 6-9 log10 PFU/mL (MOI 1-1000) in vitro. The plate was incubated at 25°C for 24 h. D: <5 h delay to reach exponential phase. N/L+: <70% ODmax. N: no effect.

tion was observed at all temperatures tested (Fig. 7A–C). This indicates that the treatment with a phage cocktail has an immediate killing effect, significantly reducing the bacterial load on chicken skin. A significant reduction in bacteria can be observed for all temperatures at 48 h. A reduction of 3.5 $\log_{10}$ CFU/cm^2 was observed at 25°C and 4°C (Fig. 7A and C) and 2.5 $\log_{10}$ CFU/cm^2 at 15°C (Fig. 7B). There was a slight increase in the bacterial load at the 12 and 24 h time-point at 25°C and 15°C (Fig. 7A and B). To investigate whether growth is due to the *in situ* emergence of phage resistance, 12 colonies from these time points were harvested and tested for phage susceptibility. No *in situ* emergence of phage resistance was observed in any of the conditions tested (data not shown). Thus, the regrowth is likely due to expansion of bacteria that were inaccessible to the phage. To further investigate if the regrowth is related to phage resistance, an *in vitro* experiment was performed in liquid culture. A final concentration of 4 $\log_{10}$ CFU/ml was treated with 5 or 7 $\log_{10}$ PFU/ml and incubated at 25°C (same conditions as biocontrol experiment). After 12 h, bacterial counts were below the detection level (100 CFU). This indicates that regrowth in the food matrix is not related to phage resistance (Figure S4, Supporting Information).

Genome-wide transduction frequency

To determine if the selected phages can horizontally transfer genomic material, a genome-wide transduction experiment was performed using a high complexity Tn5 library, with the transducing phage P22 used as a control. The library possesses single site insertions of kanamycin resistance cassette (KanR2) with a complexity of 230 K (Moraes et al. 2017, Fitzsimmons et al. 2018). This high complexity allows for screening for transduction in a genome-wide manner. All phages used in the cocktail were propagated in the Tn5 library except rfbG$_{rough}$, which does not infect this smooth strain. In all cases, an amplification >1.5 $\log_{10}$ PFU/ml was obtained to ensure > 95% represents progeny from the library (Fig. 8A). Progeny phages were used to perform a classical transduction experiment to determine the ability of phages to horizontally transfer the kanamycin resistance cassette. As shown in Fig. 8(B), CE$_{LPS}$, NP4$_{OmpC}$, and ECS$_{BtuB}$ did not produce any transductant colonies with kanamycin resistance. This suggests that these phages cannot transduce or have a frequency lower than the detection limit (1×10^{-8}). As expected, transductant colonies were obtained using phage P22 with a frequency of 1.2×10^{-6}, as reported before (Kwoh and Kemper 1978). Unexpectedly, ssTn$_{LPS}$

produced a similar number of transductant colonies compared to phage P22 ($P = .25$) (Fig. 8B). To corroborate if this transduction is due to the presence of ssTn$_{LPS}$ kanamycin transducing particles or spontaneous resistance due to phage infection, the transduction experiment was performed using phage ssTn$_{LPS}$ propagated in the S. Typhimurium ATCC14028 parental strain. ssTn$_{LPS}$ (ATCC14028) did not generate any transductant colonies since the propagation host does not possess a resistance gene for kanamycin resistance. These results suggest that ssTn$_{LPS}$ is a phage capable of carrying out transduction at low frequencies in S. Typhimurium.

Discussion

In this study, a cocktail comprised of extensively characterized phages was designed. A systematic approach was followed to include several features in the cocktail: (1) broad host range, (2) multiple-receptor recognition, (3) layered resistance approach, and (4) genetic variability of the phage.

The first step in the cocktail formulation was host range screening, which identified unique phage clusters based on phages' host range (Fig. 1). This screening also allowed to identify potential phage reisolates based on the clustering patterns. The host range of a phage can be dictated by its genotype, for example by encoding multiple receptor binding proteins, antiphage resistance proteins, and having an inherent high mutation rate (de Jonge et al. 2019). This agrees with our results, since the selected phages were representatives of different host range clusters (A, C, E, and H) and showed to be genetically distinct (Figs 1 and 6, Table 2). This suggests a direct relationship between genotype and host range in *Salmonella* phages.

The receptor screening analysis revealed that most of the selected phages (clusters A–H) use O-antigen (5/19) or BtuB (6/19) (Table 1). Similarly, Shin et al. (2012) conducted a study on the receptor diversity of 25 *Salmonella* phages and reported three types of receptors: flagella (11 phages), BtuB (seven phages), and O-antigen (seven phages). In accordance with the results of our study, they also observed that O-antigen and BtuB dependent phages showed a broader host range when compared to flagellotropic phages. The host range of the selected phages can be explained from the receptor recognition point of view. For instance, we used NTS serovars belonging to different serogroups (O:9, O:4, O:7, O:3,1, O:8, and O:1,3,19) with different somatic antigens for the host range screening (Weill 2007, Liu et al. 2014). It is possible that the O-antigen dependent phages recognize conserved LPS-moieties, such rhamnose glycans that are present in O-antigen of most of the serogroups tested. This recognition may enable infection across multiple serovars (Liu et al. 2014). Similarly, the BtuB-dependent phages selected in this study showed a broad host range. BtuB is a 614-amino acid outer membrane protein involved in the uptake of cobalamin (e.g. vitamin B$_{12}$) and has been identified as a common receptor for phages infecting *Salmonella* and *Escherichia* (Lei et al. 2011, Shin et al. 2012). This protein is highly conserved (> 90% identity) among NTS serovars (Figure S5, Supporting Information). This can explain why the BtuB-dependent phages can infect multiple NTS serovars (Shin et al. 2012). NP4$_{OmpC}$ was found to be an OmpC dependent phage (Table 1). OmpC is one of three major outer membrane proteins in Gram-negative bacteria involved in the permeability of nutrients, toxins, and antibiotics (Liu et al. 2012). Like BtuB, OmpC is highly conserved in NTS, with identities > 90% (Figure S6, Supporting Information). OmpC is a less common receptor for *Salmonella* phages compared to BtuB and O-antigen, however, it has been reported for broad host range phages such as *Salmonella*
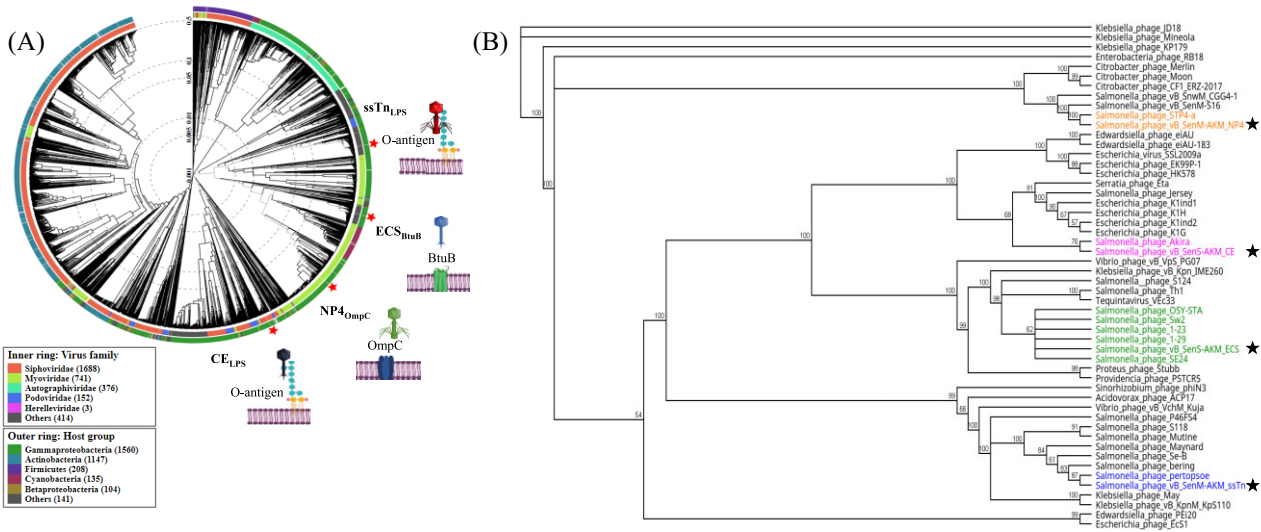
Figure 6. Phylogenetic tree of the selected *Salmonella* phages. (A) Phylogenetic tree based on all predicted CDS. Tree constructed using ViPTree version 3.1 (B) Phylogenetic tree based on the terminase large subunit amino acid sequence. The tree was generated using the Neighbor-joining method.
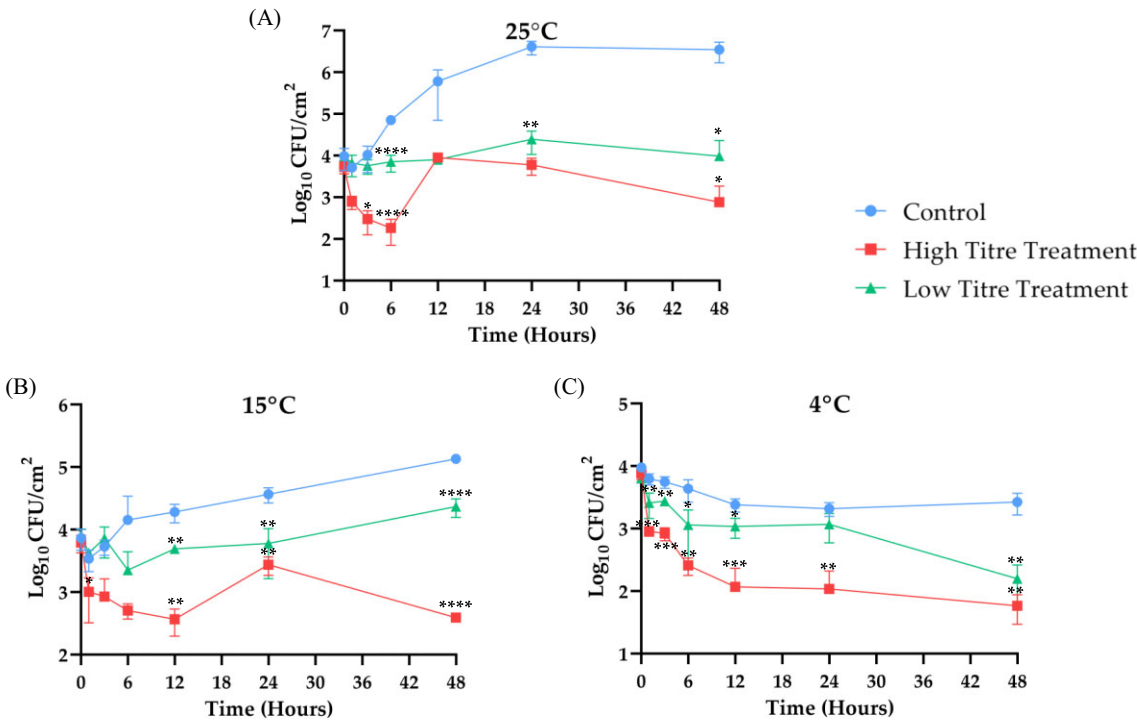

Figure 7. Biocontrol experiment on artificially inoculated chicken skin. Chicken skin pieces of 1 cm2 were artificially inoculated with 4 log10 CFU/cm2 followed by submersion into cocktail suspension containing either 5 (low titre) or 7 (high titre) log10 PFU/mL and incubated at (A) 25°C, (B) 15°C, and (C) 4°C. Data shown as means ± SD of three replicates. Bacterial counts expressed as CFU/cm2.

phage S16 (Marti et al. 2013). Screening the phage receptors allowed us to formulate a cocktail of four phages targeting distinct receptors: two O-antigen (CE$_{LPS}$ and ssTn$_{LPS}$), a BtuB (ECS$_{BtuB}$), and an OmpC (NP4$_{OmpC}$) dependent phage (Fig. 4).

The frequency of resistance emergence was quantified for all four phages (Fig. 3A). Although the BIM frequency of CE$_{LPS}$ was shown to be relatively low compared to the other phages, *S. Enteritidis* can readily generate resistance to both O-antigen dependent phages (Table S6, Supporting Information). *Salmonella* can generate resistance to O-antigen dependent phages by truncat-

ing the LPS and downregulating the expression of genes involved in LPS biosynthesis such as *lpxA*, *rfaL*, *pagP*, and *wzzB* (Santander and Robeson 2007, Wang et al. 2019). Even though O-antigen deficient *Salmonella* strains are avirulent, transient resistance can be found in strains undergoing phase variation (Santander and Robeson 2007, Cota et al. 2015). These strains can shut down the expression of the O-antigen by controlling the expression of the *opvAB* that encodes for proteins that alter the O-antigen chain length. This mechanisms allows to escape phage infection and revert to the smooth phenotype when phage challenge ceases
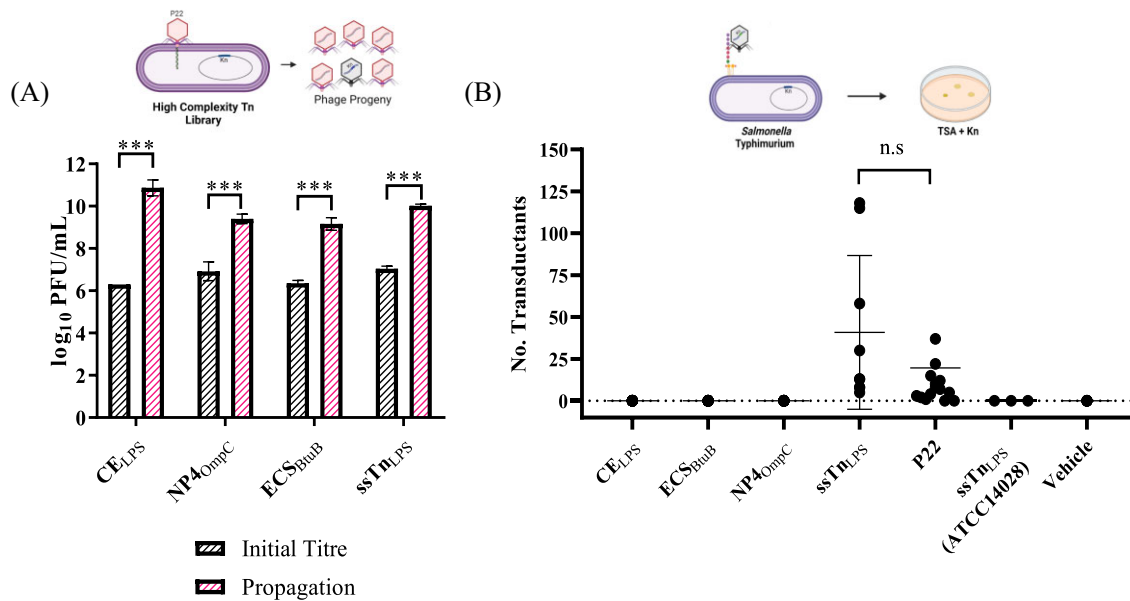
Figure 8. Genome-wide transduction experiment. (A) Phage amplification in S. Typhimurium Tn5 library. (B) Transduction experiment using phage propagated in Tn5 library. ssTnLPS (ATCC14028) was propagated in the parental strain S. Typhimurium ATCC14028.

(Cota et al. 2015). $rfbG_{rough}$ was able to infect some of the CE_{LPS} and $ssTn_{LPS}$ resistant mutants with an EOP of 1 (Fig. 3B; Table S6, Supporting Information). This phage was only able to infect O-antigen deficient *Salmonella* strains, something characteristic of rough specific phages. Kim et al. (2014) reported a rough specific phage SSU5, like our study, this phage was only able to infect rough *Salmonella* strains, targeting the core LPS moiety. The combination of SSU5 with the O-antigen dependent phage, SSU14, significantly reduced the emergence of resistance compared to single phage treatment. Therefore, the addition of $rfbG_{rough}$ auxiliary phage adds an additional level of infection known as "layered" cocktail, previously reported using *Klebsiella* phages (Hesse et al. 2020). To identify receptor of phage $rfbG_{rough}$, double knockout mutants of $\Delta rfaL$ and $\Delta fhuA$, $\Delta fliC$, $\Delta flgE$, or $\Delta ompA$ were used. The EOP of $rfbG_{rough}$ was reduced in the $\Delta rfaL\Delta ompA$ mutant, suggesting that OmpA is important for the infection of this phage (Figure S7, Supporting Information). However, more experiments are needed to verify these results.

Despite our efforts, phage $rfbG_{rough}$ showed recalcitrance to sequencing using the Illumina platform. Future tests will explore techniques like generating creating cDNA libraries by RT-PCR or RNA-Seq-based genome assembly for phage genome reconstruction (Haas et al. 2013). Furthermore, the four sequenced phages showed to be genetically distinct belonging (Fig. 6 and Table 2). The use of genomically distinct phages in a cocktail is favorable to avoid the generation of cross-resistance with mechanisms like CRISPR–Cas (Ross et al. 2016). Hynes et al. (2014) demonstrated that *Streptococcus thermophilus* can develop cross-resistance to both phage 858 and 2972 (90.9% identical) by the acquisition of spacer(s) from phage 858. Moreover, it has been reported that phages encoding for anti-CRISPR genes can cooperate during infection to overcome CRISPR mechanisms. During this cooperation, one phage blocks the host CRISPR–Cas to allow the replication of the second phage (Landsberger et al. 2018). These observations are consistent with the cross-resistance assay results where cross-resistance to all phages was not observed in BIMs isolated from single phage treatment (Fig. 3B). The significantly lower BIM frequency of the cocktail compared to single

phage treatment can be attributed to similar cooperative phage interactions (Fig. 3A).

Chicken skin was used in this study to evaluate the antimicrobial effect of the *Salmonella* phage cocktail. This matrix was selected to simulate: (1) the contamination of chicken skin in final chicken carcasses and cuts, and (2) the recommended use of phages at the last stage of processing to minimize recontamination (Carter et al. 2012, Moye et al. 2018). *Salmonella* is highly prevalent on chicken skin due to its tight attachment and the inaccessibility of chemical disinfectants with concentrations ranging from 2.5 to 3.1 log_{10} CFU/g (Guran et al. 2017, Rimet et al. 2019, Oh et al. 2023). In this study, the chicken skin was inoculated to a final concentration of 4 log_{10} CFU/cm^2 (2.5–3.5 log_{10} CFU/g) to mimic naturally contaminated chicken skin and testing conditions of commercially available phage products (Sukumaran et al. 2016). The cocktail treatment, applied at a concentration of 7 log_{10} PFU/ml, resulted in a 3.5 log_{10} CFU/cm^2 reduction after 48 h at both 25°C and 15°C, and a 2.5 log_{10} CFU/cm^2 reduction at 4°C, compared to the control (Fig. 7). A virucide solution was used during sample recovery to remove residual phage. The virucide solution completely inactivated the phages when standardized to a concentration of 8 log_{10} PFU/ml, without affecting the bacterial counts (Figure S8, Supporting Information). This is an important step to prevent bacterial reductions during sample recovery and overestimation of the phage efficacy (Dhowlaghar and Denes 2023). A study performed in raw beef showed that residual phage was able to lyse over 50% of *E. coli* O157: H7 populations during the rinsing step (Liu et al. 2015). In the present experiment, since a virucide solution was added during sample recovery, the observed reductions are considered *in situ*. Interestingly, despite the large reduction in bacterial load at 48 h, there was a transient slight increase in the bacterial load at the 12 and 24 h time-point at 25°C and 15°C (Fig. 7A and B). The observed regrowth could be attributed to two phenomena: (1) the complexity of the chicken surface or (2) the bacteria population reached a threshold concentration of spatial refuge. Chicken skin is rich in feather follicles where bacteria can absorb and hinder the accessibility of antimicrobials (Zhang et al. 2020). Additionally, the

chicken skin samples used in this experiment were not disinfected as is commonly performed in the literature, this can also contribute to the complexity of the matrix due to the presence of natural skin microbiota (Hungaro et al. 2013, Lee et al. 2014, Bai et al. 2019, Islam et al. 2021). On the other hand, the bacterial reduction caused by the phage treatment may have reduced the bacterial population to sufficiently low concentration to achieve spatial refuge. After 24 h, the bacterial concentration reached surpasses the spatial refuge, thus allowing phage infection and subsequent reduction in the bacterial counts (Fig. 7) (Schrag and Mittler 1996).

Ideal candidate phages for therapy and biocontrol should display a low transduction potential (Islam et al. 2021). Although transduction is undesirable in phages used for biocontrol, it is commonly observed in natural lytic phages (Al-Anany et al. 2021). Generalized transduction has been considered challenging to avoid and inevitable in some cases (Monteiro et al. 2019, Al-Anany et al. 2021). Despite its importance, the transduction capabilities of phages are often overlooked in recent literature (Islam et al. 2019, Anjay et al. 2022, Pan et al. 2023). Methods to quantify phage-mediated transduction often involve the utilization of genetic elements, such as antibiotic resistance or metabolically essential genes. These genes may be encoded either chromosomally or in plasmids, and their transduction can be influenced by the genomic locus or nucleotide sequence (Marti et al. 2013, Mašlaňová et al. 2016). This can potentially overlook some transduction mechanisms that are sequence dependent such as the pac-dependent transduction of phage P22 (Chiang et al. 2019). We showed here that using a high-complexity transposon library (Moraes et al. 2017, Fitzsimmons et al. 2018) can be a powerful tool to quantify phage transduction. Using a complex transposon library allows transduction at tens of thousands of locations to be assessed by the transfer of antibiotic resistance, thereby maximizing the probability of identifying transduction events. This method has been used previously by Bowring et al. (2022) to study and quantify the lateral and specialized transduction of *Staphylococcus aureus* prophage ϕ11. We demonstrated here that this method can be adapted to lytic *Salmonella* phages belonging to different families, subfamilies and morphotypes.

Conclusions

In conclusion, the systematic approach used in this study to develop a new *Salmonella* phage cocktail was successful. The cocktail showed a broad inhibition spectrum against all NTS strains tested with low emergence of resistance in *S*. Enteritidis. A lack of transduction was shown for three of the four phages. Genomic characterization demonstrated the absence of virulence factors or AMR genes, indicating that these phages are safe for biocontrol. Moreover, the phage cocktail showed bactericidal and bacteriostatic effects on chicken skin, indicating its feasibility in controlling *Salmonella* in poultry products. Lastly, we showed extensive phenotypic and genotypic characterization of these phages, providing a characterization standard for the phage scientific community.

Acknowledgments

Supplementary data

Supplementary data is available at *FEMSML Journal* online.

Conflict of interest: None declared.

References

Adams MH. *Bacteriophages*. New York, London: Interscience Publishers, 1959.

Al-Anany AM, Fatima R, Hynes AP. Temperate phage-antibiotic synergy eradicates bacteria through depletion of lysogens. *Cell Rep* 2021;**35**:109172.

Anjay KA, Abhishek MH, Dubal ZB *et al.* Isolation and characterization of *Salmonella* phages and phage cocktail mediated biocontrol of *Salmonella enterica* serovar Typhimurium in chicken meat. *LWT* 2022;**155**:112957.

Atterbury RJ, Gigante AM, Rubio Lozano MdlS M *et al.* Reduction of *Salmonella* contamination on the surface of chicken skin using bacteriophage. *Virol J* 2020;**17**:98.

Bai J, Jeon B, Ryu S. Effective inhibition of *Salmonella* typhimurium in fresh produce by a phage cocktail targeting multiple host receptors. *Food Microbiol* 2019;**77**:52–60.

Bankevich A, Nurk S, Antipov D *et al.* SPAdes: a new genome assembly algorithm and its applications to single-cell sequencing. *J Comput Biol* 2012;**19**:455–77.

Basler C, Nguyen T-A, Anderson TC *et al.* Outbreaks of human *Salmonella* infections associated with live poultry, United States, 1990-2014. *Emerg Infect Dis* 2016;**22**:1705–11.

Bowring JZ, Su Y, Alsaadi A *et al.* Screening for highly transduced genes in *Staphylococcus aureus* revealed both lateral and specialized transduction. *Microbiol Spectr* 2022;**10**: e0242321.

Calva E, Silva C, Zaidi MB *et al.* Complete genome sequencing of a multidrug-resistant and human-invasive *Salmonella* enterica serovar typhimurium strain of the emerging sequence type 213 genotype. *Genome Announc* 2015;**3**: e00663–15.

Carter CD, Parks A, Abuladze T *et al.* Bacteriophage cocktail significantly reduces *Escherichia coli* O157: H7 contamination of lettuce and beef, but does not protect against recontamination. *Bacteriophage* 2012;**2**:178–85.

Caruso SM, deCarvalho TN, Huynh A *et al.* A novel genus of actinobacterial tectiviridae. *Viruses* 2019;**11**:1134.

CDC. *Foodborne Germs and Illnesses*. Vol. **2023**. Atlanta: CDC, 2023. https://www.cdc.gov/foodsafety/foodborne-germs.html. (10 October 2023, date last accessed).

CDC. *Reports of Selected Salmonella Outbreak Investigations*. Vol. **2021**. Atlanta: CDC, 2020a. https://www.cdc.gov/salmonella/outbreaks.html. (21 March 2021, date last accessed).

CDC. *Reports of Selected Salmonella Outbreak Investigations*. Vol. **2020**. Atlanta: Centers for Disease Control and Prevention, 2020b.

Chiang YN, Penadés JR, Chen J. Genetic transduction by phages and chromosomal islands: the new and noncanonical. *PLoS Pathog* 2019;**15**:e1007878.

Chibeu A, Balamurugan S. Application of a virucidal agent to avoid overestimation of phage kill during phage decontamination assays on ready-to-eat meats. *Methods Mol Biol* 2018;**1681**: 97–105.

Clavijo V, Baquero D, Hernandez S *et al.* Phage cocktail SalmoFREE® reduces *Salmonella* on a commercial broiler farm. *Poult Sci* 2019;**8**:5054–63.

Cota I, Sánchez-Romero MA, Hernández SB *et al.* Epigenetic control of *Salmonella enterica* O-antigen chain length: a tradeoff between virulence and bacteriophage resistance. *PLoS Genet* 2015;**11**:e1005667.

de Jonge PA, Nobrega FL, Brouns SJJ *et al.* Molecular and evolutionary determinants of bacteriophage host range. *Trends Microbiol* 2019;**27**:51–63.

Dhowlaghar N, Denes TG. Control of residual phage in the evaluation of phage-based food safety applications. *Crit Rev Food Sci Nutr* 2023;**14**:1–7.

Dunne M, Denyes JM, Arndt H *et al. Salmonella* phage S16 tail fiber adhesin features a rare polyglycine rich domain for host recognition. *Structure* 2018;**26**:1573–82.e4.

. Economic Research Service USDoA. . *Cost Estimates of Foodborne Illnesses* Hoffman S. (ed.), Vol. **2022**, In: Washington: U.S Department of Agriculture, 2022.

Efimov AD, Golomidova AK, Kulikov EE *et al.* RB49-like bacteriophages recognize O antigens as one of the alternative primary receptors. *Int J Mol Sci* 2022;**23**:11329.

El-Dougdoug NK, Cucic S, Abdelhamid AG *et al.* Control of *Salmonella* Newport on cherry tomato using a cocktail of lytic bacteriophages. *Int J Food Microbiol* 2019;**93**:60–71.

Emond-Rheault JG, Jeukens J, Freschi L *et al.* A Syst-OMICS approach to ensuring food safety and reducing the economic burden of salmonellosis. *Front Microbiol* 2017;**8**:996.

Ferrari RG, Rosario DKA, Cunha-Neto A *et al.* Worldwide epidemiology of *Salmonella* serovars in animal-based foods: a meta-analysis. *Appl Environ Microb* 2019;**85**:e00591–00519.

Fitzsimmons L, Liu L, Porwollik S *et al.* Zinc-dependent substrate-level phosphorylation powers *Salmonella* growth under nitrosative stress of the innate host response. *PLoS Pathog* 2018;**14**: e1007388.

Fox KL, Srikhanta YN, Jennings MP. Phase variable type III restriction-modification systems of host-adapted bacterial pathogens. *Mol Microbiol* 2007;**65**:1375–9.

Gao D, Ji H, Wang L *et al.* Fitness trade-offs in phage cocktail-resistant *Salmonella enterica* serovar *enteritidis* results in increased antibiotic susceptibility and reduced virulence. *Microbiol Spectr* 2022;**10**:e02914–02922.

Goode D, Allen VM, Barrow PA. Reduction of experimental *Salmonella* and *Campylobacter* contamination of chicken skin by application of lytic bacteriophages. *Appl Environ Microb* 2003;**69**:5032–6.

Goulet A, Spinelli S, Mahony J *et al.* Conserved and diverse traits of adhesion devices from *Siphoviridae* recognizing proteinaceous or saccharidic receptors. *Viruses* 2020;**12**:512.

Grant AQ, Parveen S, Schwarz J *et al.* Reduction of *Salmonella* in ground chicken using a bacteriophage. *Poult Sci* 2017;**6**:2845–52.

Guenther S, Huwyler D, Richard S *et al.* Virulent bacteriophage for efficient biocontrol of *Listeria monocytogenes* in ready-to-eat foods. *Appl Environ Microb* 2009;**5**:93–100.

Guran HS, Mann D, Alali WQ. Salmonella prevalence associated with chicken parts with and without skin from retail establishments in Atlanta metropolitan area, Georgia. *Food Contr* 2017;**73**:462–7.

Haas BJ, Papanicolaou A, Yassour M *et al.* De novo transcript sequence reconstruction from RNA-seq using the Trinity platform for reference generation and analysis. *Nat Protoc* 2013;**8**:1494–512.

Harvey PC, Watson M, Hulme S *et al. Salmonella enterica* serovar typhimurium colonizing the lumen of the chicken intestine grows slowly and upregulates a unique set of virulence and metabolism genes. *Infect Immun* 2011;**79**:4105–21.

Hesse S, Rajaure M, Wall E *et al.* Phage resistance in multidrug-resistant *Klebsiella* pneumoniae ST258 evolves via diverse mutations that culminate in impaired adsorption. *mBio* 2020;**11**:e02530–19.

Higgins JP, Higgins SE, Guenther KL *et al.* Use of a specific bacteriophage treatment to reduce *Salmonella* in poultry products. *Poult Sci* 2005;**84**:1141–5.

Hoffmann S, Batz MB, Morris JG. Annual cost of illness and quality-adjusted life year losses in the united states due to 14 foodborne pathogens. *J Food Prot* 2012;**5**:1292–302.

Hungaro HM, Mendonça RCS, Gouvêa DM *et al.* Use of bacteriophages to reduce *Salmonella* in chicken skin in comparison with chemical agents. *Food Res Int* 2013;**52**:75–81.

Hynes AP, Villion M, Moineau S. Adaptation in bacterial CRISPR-Cas immunity can be driven by defective phages. *Nat Commun* 2014;**5**:4399.

Islam MR, Martinez-Soto CE, Lin JT *et al.* A systematic review from basics to omics on bacteriophage applications in poultry production and processing. *Crit Rev Food Sci Nutr* 2021;**63**:1–33.

Islam MS, Zhou Y, Liang L *et al.* Application of a phage cocktail for control of *Salmonella* in foods and reducing biofilms. *Viruses* 2019;**1**:841.

Jain S, Mukhopadhyay K, Thomassin PJ. An economic analysis of *Salmonella* detection in fresh produce, poultry, and eggs using whole genome sequencing technology in Canada. *Food Res Int* 2019;**116**:802–9.

Kanamaru S, Ishiwata Y, Suzuki T *et al.* Control of bacteriophage T4 tail lysozyme activity during the infection process. *J Mol Biol* 2005;**346**:1013–20.

Kang HW, Kim JW, Jung TS *et al.* wksl3, a new biocontrol agent for *Salmonella* enterica serovars Enteritidis and Typhimurium in foods: characterization, application, sequence analysis, and oral acute toxicity study. *Appl Environ Microb* 2013;**9**:1956–68,

Kim M, Kim S, Park B *et al.* Core lipopolysaccharide-specific phage SSU5 as an auxiliary component of a phage cocktail for *Salmonella* biocontrol. *Appl Environ Microb* 2014;**80**:1026–34.

Kim M, Ryu S. Characterization of a T5-like coliphage, SPC35, and differential development of resistance to SPC35 in *Salmonella* enterica serovar Typhimurium and *Escherichia coli*. *Appl Environ Microb* 2011;**77**:2042–50.

Kropinski AM, Mazzocco A, Waddell TE *et al.* Enumeration of bacteriophages by double agar overlay plaque assay. *Methods Mol Biol* 2009;**501**:569–76.

Kropinski AM. Measurement of the rate of attachment of bacteriophage to cells. *Methods Mol Biol* 2009;**501**:569–76.

Kruk ZA, Kim HJ, Kim YJ *et al.* Combined effects of high pressure processing and addition of soy sauce and olive oil on safety and quality characteristics of chicken breast meat. *Asian Australas J Anim Sci* 2014;**27**:256–65.

Kwoh DY, Kemper J. Bacteriophage P22-mediated specialized transduction in *Salmonella* Typhimurium: high frequency of aberrant prophage excision. *J Virol* 1978;**27**:519–34.

Landsberger M, Gandon S, Meaden S *et al.* Anti-CRISPR phages cooperate to overcome CRISPR-Cas immunity. *Cell* 2018;**174**:908–16.e12.

Lee NY, Park SY, Kang IS *et al.* The evaluation of combined chemical and physical treatments on the reduction of resident microorganisms and *Salmonella* typhimurium attached to chicken skin. *Poult Sci* 2014;**3**:208–15.

Lei G-S, Syu W, Liang P-H *et al*. Repression of btuB gene transcription in *Escherichia coli* by the GadX protein. *BMC Microbiol* 2011;**11**:33.

Lin DM, Koskella B, Lin HC. Phage therapy: an alternative to antibiotics in the age of multi-drug resistance. *WJGPT* 2017;**8**:162.

Liu B, Knirel YA, Feng L *et al*. Structural diversity in *Salmonella* O antigens and its genetic basis. *FEMS Microbiol Rev* 2014;**38**:56–89.

Liu B, Zheng D, Jin Q *et al*. VFDB 2019: a comparative pathogenomic platform with an interactive web interface. *Nucleic Acids Res* 2019;**47**:D687–92.

Liu H, Meng R, Wang J *et al*. Inactivation of *Escherichia coli* O157 bacteriophages by using a mixture of ferrous sulfate and tea extract. *J Food Prot* 2015;**78**:2220–6.

Liu W, Han L, Song P *et al*. Complete genome sequencing of a Tequintavirus bacteriophage with a broad host range against *Salmonella* Abortus equi isolates from donkeys. *Front Microbiol* 2022;**13**:938616.

Liu YF, Yan JJ, Lei HY *et al*. Loss of outer membrane protein C in *Escherichia coli* contributes to both antibiotic resistance and escaping antibody-dependent bactericidal activity. *Infect Immun* 2012;**80**:1815–22.

MacLachlan PR, Kadam SK, Sanderson KE. Cloning, characterization, and DNA sequence of the rfaLK region for lipopolysaccharide synthesis in *Salmonella* Typhimurium LT2. *J Bacteriol* 1991;**73**:7151–63.

Marti R, Zurfluh K, Hagens S *et al*. Long tail fibres of the novel broad-host-range T-even bacteriophage S16 specifically recognize *Salmonella* OmpC. *Mol Microbiol* 2013;**87**:818–34.

Martinez-Soto CE, Cucić S, Lin JT *et al*. PHIDA: a high throughput turbidimetric data analytic tool to compare host range profiles of bacteriophages isolated using different enrichment methods. *Viruses* 2021;**13**:2120.

Mašlaňová I, Stříbná S, Doškař J *et al*. Efficient plasmid transduction to *Staphylococcus aureus* strains insensitive to the lytic action of transducing phage. *FEMS Microbiol Lett* 2016;**363**:fnw211.

McArthur AG, Waglechner N, Nizam F *et al*. The comprehensive antibiotic resistance database. *Antimicrob Agents Chemother* 2013;**57**:3348–57.

McGinnis S, Madden TL. BLAST: at the core of a powerful and diverse set of sequence analysis tools. *Nucleic Acids Res* 2004;**32**:W20–5.

McNair K, Bailey BA, Edwards RA. PHACTS, a computational approach to classifying the lifestyle of phages. *Bioinformatics* 2012;**28**:614–8.

Millman A, Bernheim A, Stokar-Avihail A *et al*. Bacterial retrons function in anti-phage defense. *Cell* 2020;**183**:1551–61.e12.

Monteiro R, Pires DP, Costa AR *et al*. Phage therapy: going temperate?. *Trends Microbiol* 2019;**27**:368–78.

Moraes MH, Desai P, Porwollik S *et al*. *Salmonella* persistence in tomatoes requires a distinct set of metabolic functions identified by transposon insertion sequencing. *Appl Environ Microb* 2017;**83**:e03028–03016.

Moreno Swift AI, den Bakker HC, Vongkamjan K *et al*. *Salmonella* bacteriophage diversity reflects host diversity on dairy farms. *Food Microbiol* 2013;**6**:275–85.

Moye ZD, Woolston J, Sulakvelidze A. Bacteriophage applications for food production and processing. *Viruses* 2018;**10**:1–22.

Nishimura Y, Yoshida T, Kuronishi M *et al*. ViPTree: the viral proteomic tree server. *Bioinformatics* 2017;**33**:2379–80.

Oh H, Yoon Y, Yoon JW *et al*. Salmonella risk assessment in poultry meat from farm to consumer in Korea. *Foods* 2023;**12**:649.

Oksanen HM., Ictv Report C. ICTV virus taxonomy profile: corticoviridae. *J Gen Virol* 2017;**98**:888–9.

Ortega Morente E, Fernández-Fuentes MA, Grande Burgos MJ *et al*. Biocide tolerance in bacteria. *Int J Food Microbiol* 2013;**162**:13–25.

Pan H, Shu M, Li T-J *et al*. Isolation and characterization of two lytic phages against multidrug-resistant Salmonella and their application as a cocktail for biocontrol in foods. *LWT* 2023;**185**:115184.

Park M, Lee JH, Shin H *et al*. Characterization and comparative genomic analysis of a novel bacteriophage, SFP10, simultaneously inhibiting both *Salmonella* enterica and *Escherichia coli* O157:H7. *Appl Environ Microb* 2012;**78**:58–69.

PHAC. *FoodNet Canada Annual Report 2017*. Ottawa: FoodNet Canada publications, 2017, 47–47.

Phagelux. FDA. https://www.fda.gov/media/95017/download Phagelux GRAS Application for SalmoPro®. 2020.

Radovčić NM, Ježek D, Markov K *et al*. The effect of high pressure treatment on the quality of chicken breast meat. *Croatian J of Food Tech* 2019;**14**:76–81.

Ramsey J, Rasche H, Maughmer C *et al*. Galaxy and Apollo as a biologist-friendly interface for high-quality cooperative phage genome annotation. *PLoS Comput Biol* 2020;**16**:e1008214.

Rimet C-S, Maurer JJ, Pickler L *et al*. *Salmonella* harborage sites in infected poultry that may contribute to contamination of ground meat. 2019;**3**. https://doi.org/10.3389/fsufs.2019.00002.

Ross A, Ward S, Hyman P. More is better: selecting for broad host range bacteriophages. *Front Microbiol* 2016;**7**. https://doi.org/10.3389/fmicb.2016.01352.

Salmond GPC, Fineran PC. A century of the phage: past, present and future. *Nat Rev Micro* 2015;**13**:777–86.

Santander J, Robeson J. Phage-resistance of *Salmonella* enterica serovar Enteritidis and pathogenesis in *Caenorhabditis elegans* is mediated by the lipopolysaccharide. *Electron J Biotechnol* 2007;**10**:0–0.

Santiviago CA, Reynolds MM, Porwollik S *et al*. Analysis of pools of targeted *Salmonella* deletion mutants identifies novel genes affecting fitness during competitive infection in mice. *PLoS Pathog* 2009;**5**:e1000477.

Schrag SJ, Mittler JE. Host-parasite coexistence: the role of spatial refuges in stabilizing bacteria-phage interactions. *Am Nat* 1996;**148**:348–77.

Shariat N, Timme RE, Pettengill JB *et al*. Characterization and evolution of *Salmonella* CRISPR-Cas systems. *Microbiology* 2015;**161**:374–86.

Sher AA, Mustafa BE, Grady SC *et al*. Outbreaks of foodborne *Salmonella* enteritidis in the United States between 1990 and 2015: an analysis of epidemiological and spatial-temporal trends. *IJID* 2021;**105**:54–61.

Shin H, Lee J-H, Kim H *et al*. Receptor diversity and host interaction of bacteriophages infecting *Salmonella* enterica serovar Typhimurium. *PLoS ONE* 2012;**7**:e43392.

Spricigo DA, Bardina C, Cortés P *et al*. Use of a bacteriophage cocktail to control *Salmonella* in food and the food industry. *Int J Food Microbiol* 2013;**65**:169–74,

Su LH, Chiu CH. *Salmonella*: clinical importance and evolution of nomenclature. *CGMH* 2007;**30**:210–9.

Sukumaran AT, Nannapaneni R, Kiess A *et al*. Reduction of *Salmonella* on chicken breast fillets stored under aerobic or modified atmosphere packaging by the application of lytic bacteriophage preparation SalmoFreshTM. *Poult Sci* 2016;**95**:668–75.

Sukumaran AT, Nannapaneni R, Kiess A *et al*. Reduction of *Salmonella* on chicken meat and chicken skin by combined or sequential application of lytic bacteriophage with chemical antimicrobials. *Int J Food Microbiol* 2015;**207**:8–15.

Theuß T, Woitow G, Bulang M *et al*. Demonstration of the efficacy of a *Salmonella* Enteritidis live vaccine for chickens accord-

ing to the current European Pharmacopoeia Monograph. *Heliyon* 2018;**4**:e01070.

Thomas MK, Murray R, Flockhart L *et al.* Estimates of foodborne illness-related hospitalizations and deaths in Canada for 30 specified pathogens and unspecified agents. *Foodborne Pathog Dis* 2015;**12**:820–7.

Thomas MK, Murray R, Flockhart L *et al.* Estimates of the burden of foodborne illness in Canada for 30 specified pathogens and unspecified agents, Circa 2006. *Foodborne Pathog Dis* 2013;**10**:639–48.

Vander Byl C, Kropinski AM. Sequence of the genome of Salmonella bacteriophage P22. *J Bacteriol* 2000;**182**:6472–81.

Wahl A, Battesti A, Ansaldi M. Prophages in *Salmonella enterica*: a driving force in reshaping the genome and physiology of their bacterial host?. *Mol Microbiol* 2019;**111**:303–16.

Walter M, Fiedler C, Grassl R *et al.* Structure of the receptor-binding protein of bacteriophage det7: a podoviral tail spike in a myovirus. *J Virol* 2008;**82**:2265–73.

Wang C, Nie T, Lin F *et al.* Resistance mechanisms adopted by a *Salmonella* Typhimurium mutant against bacteriophage. *Virus Res* 2019;**273**:197759.

Weill PADGF-X. *Antigenic Formulae of the Salmonella Serovars*. Vol. **9**. Paris: WHO Collaborating Centre for Reference and Research on Salmonella, 2007, 167.

Whichard JM, Sriranganathan N, Pierson FW. Suppression of *Salmonella* growth by wild-type and large-plaque variants of bacteriophage Felix O1 in liquid culture and on chicken frankfurters. *J Food Prot* 2003;**66**: 220–5.

Whichard JM, Weigt LA, Borris DJ *et al.*, Complete genomic sequence of bacteriophage felix o1. *Viruses* 2010;**2**:710–30. https://doi.org/10.3390/v2030710.

Wollin R, Eriksson U, Lindberg AA. *Salmonella* bacteriophage glycanases: endorhamnosidase activity of bacteriophages P27, 9NA, and KB1. *J Virol* 1981;**38**:1025–33.

Yehl K, Lemire S, Yang AC *et al.* Engineering phage host-range and suppressing bacterial resistance through phage tail Fiber mutagenesis. *Cell* 2019;**179**: 459–69.e9.

Yimenu SM, Koo J, Kim BS *et al.* Freshness-based real-time shelf-life estimation of packaged chicken meat under dynamic storage conditions. *Poult Sci* 2019;**98**:6921–30.

Yu P, Mathieu J, Li M *et al.* Isolation of polyvalent bacteriophages by sequential multiple-host approaches. *Appl Environ Microb* 2016;**2**:808–15.

Zhang X, Peng Z, Li P *et al.* Complex internal microstructure of feather follicles on chicken skin promotes the bacterial cross-contamination of carcasses during the slaughtering process. *Front Microbiol* 2020;**11**:571913.

Zinno P, Devirgiliis C, Ercolini D *et al.* Bacteriophage P22 to challenge *Salmonella* in foods. *Int J Food Microbiol* 2014;**91**:69–74.